macaques were euthanized at 13 dpi and the other two were euthanized at 26 dpi. Two of the adult macaques were euthanized at 13 dpi and one adult macaque was euthanized at 27 dpi. The remaining four monkeys (two newborns and two adults) were used as age-matched uninfected controls.

Sample collection. Blood samples were periodically collected from all monkeys, treated with sodium citrate as an anticoagulant, and centrifuged to obtain plasma. Peripheral blood mononuclear cells (PBMCs) were separated from the buffy coat by Percoll (Lymphocyte Separation Solution; Nacalai Tesque, Kyoto, Japan) density gradient centrifugation. Separated plasma and PBMCs were stored at −80 C until use. Thymus, spleen and mesenteric lymph nodes were obtained at the time of necropsy, and minced and filtered through a 40 μm nylon filter (Becton Dickinson, Franklin Lakes, N.J., U.S.A.). These single cell suspension samples were divided and used for plaque assay and DNA extraction.

Measurement of viral loads. Plasma viral RNA levels were determined by real-time PCR (Prism 7700 Sequence Detector, Applied Biosystems, Foster City, Calif., U.S.A.) as described previously (27). The proviral DNA loads in PBMC and thymocytes were determined by quantitative PCR. RNA-free DNA samples were extracted from 2×10^6 cells with a QIAGEN DNeasy Tissue kit (QIAGEN, Hilden, Germany). PCR was performed with a Platinum qRT-PCR ThermoScript One-Step System (Invitrogen, Carlsbad, Calif., U.S.A.) using the same primer set and probe that were used in RT-PCR. A standard curve was generated from a plasmid DNA sample containing the full genome of KS661, which was quantified with a UV-spectrophotometer. Infectious viral roads in several lymphoid tissues were quantified using the infectious plaque assay as described previously (33).

Flow cytometry analysis. The frequency of $CD4^+$ T cells in whole bloods was examined as described previously (32). Thymocytes were stained for flow cytometry using the panel of monoclonal antibodies (mAbs) shown in Table 1. Cells were adjusted to a concentration of 10^6 cells/100 μl, stained using appropriately diluted antibody for 30 min at 4 C, washed, fixed with Cellfix (BD Biosciences, San Jose, Calif., U.S.A.), and analyzed with a FACScan or FACSCalibur analyzer (BD Biosciences). Thymocytes whose surface had already been stained were fixed with 1% formaldehyde, incubated with FACS permeabilization solution 2 (BD Biosciences) for 10 min, stained in the dark for 30 min with mAb against terminal deoxynucleotidyl transferase (TdT) or isotype-matched control (BD Biosciences), washed, resuspended in Cellfix and analyzed with the FACSCalibur analyzer.

Cell surface staining and cell sorting of obtained thymocytes. Cells were surface stained and TN cells were sorted as previously described (11). Thymocytes were stained with FITC-anti-monkey CD3, PE-anti-human CD4, APC-anti-human CD8 (Leu-2a; BD Biosciences) and 7-AAD Viability Dye (Coulter, Miami, Fla., U.S.A.). $CD3^-CD4^-CD8^-$ TN cells were sorted by FACSVantageSE (BD Biosciences). Non-lymphoid cells were excluded by forward and side scatters. Non-viable cells were excluded using 7-AAD Viability Dye. Sorted cells were reanalyzed to check their purity and were always found to be more than 99% pure.

Mice and fetal thymus organ culture (FTOC). Pregnant C57BL/6 (B6) mice were purchased from Japan SLC (Shizuoka, Japan). B6 fetuses (15 days post-coitum) were used in organ culture experiments as the source of fetal thymus lobes. Fetal thymus lobes were cultured as described previously (53) with subsequent modifications (23). One murine thymus lobe and 2,000 cells of $CD3^-CD4^-CD8^-$ TN monkey thymocytes purified by the cell sorter were added to each well into a total volume of 200 μl. Wells along the margin of the plate were not used, but filled with water to help maintain a high humidity in the plate. The plates were centrifuged at $150\times g$ for 5 min at room temperature, placed into a plastic bag (Ohmi Oder Air Service,

Table 1. Combinations of monoclonal antibodies used in the FACS analysis

Antibody combination	Labeled fluorescence			
	FITC[a]	PE[b]	PerCP[c]	APC[d]
1	CD2[e]	CD4[f]	CD3[g]	CD8[h]
2	CD11b[i]	CD4	CD3	CD8
3	CD16[j]	CD4	CD3	CD8
4	CD20[k]	CD4	CD3	CD8
5	CD4[f]	CD56[l]	CD3	CD8
6	TdT[m]	CD4	CD3	CD8

[a] Fluorescein isothiocyanate.
[b] Phycoerythrin.
[c] Peridinin chlorophyll protein.
[d] Allophycocyanin.
[e] Clone 39c1.5; Coulter, Miami, Fla., U.S.A.
[f] Clone Nu-Th/i; Nichirei, Tokyo.
[g] Anti-CD3 reagent (FN-18; Biosource, Camarillo, Calif., U.S.A.) was biotinylated, and a two-step staining procedure was performed using streptavidin PerCP (BD Biosciences Pharmingen) as the secondary reagent.
[h] Clone SK1; BD Biosciences, San Jose, Calif., U.S.A.
[i] Clone Bearl: Coulter, Miami, Fla., U.S.A.
[j] Clone 3G8; Coulter, Miami, Fla., U.S.A.
[k] Clone L27; BD Biosciences, San Jose, Calif., U.S.A.
[l] Clone B159; BD Biosciences, San Jose, Calif., U.S.A.
[m] Anti-terminal deoxynucleotidyl transferase reagent for detecting intracellular epitopes. It is a mixture of four monoclonal antibodies (HT1, HT4, HT8 and HT9; Beckman Coulter, Miami, Fla., U.S.A.).

Hikone, Japan), and the air inside was replaced by a gas mixture (70% O_2, 25% N_2 and 5% CO_2). The plastic bag was incubated at 37 C. The cultures were maintained in RPMI 1640 medium. The medium was changed every 2 or 3 days. Cells from both inside and outside the lobe were harvested from each well at each time point, and single cell suspensions were made. Viable cells were counted by trypan blue dye exclusion, and then surface phenotypes were analyzed by FACSVantageSE.

Histopathological and immunohistochemical examinations. The thymuses obtained from sacrificed monkeys were fixed in 4% paraformaldehyde and 1× phosphate-buffered saline overnight at 4 C, and then embed-

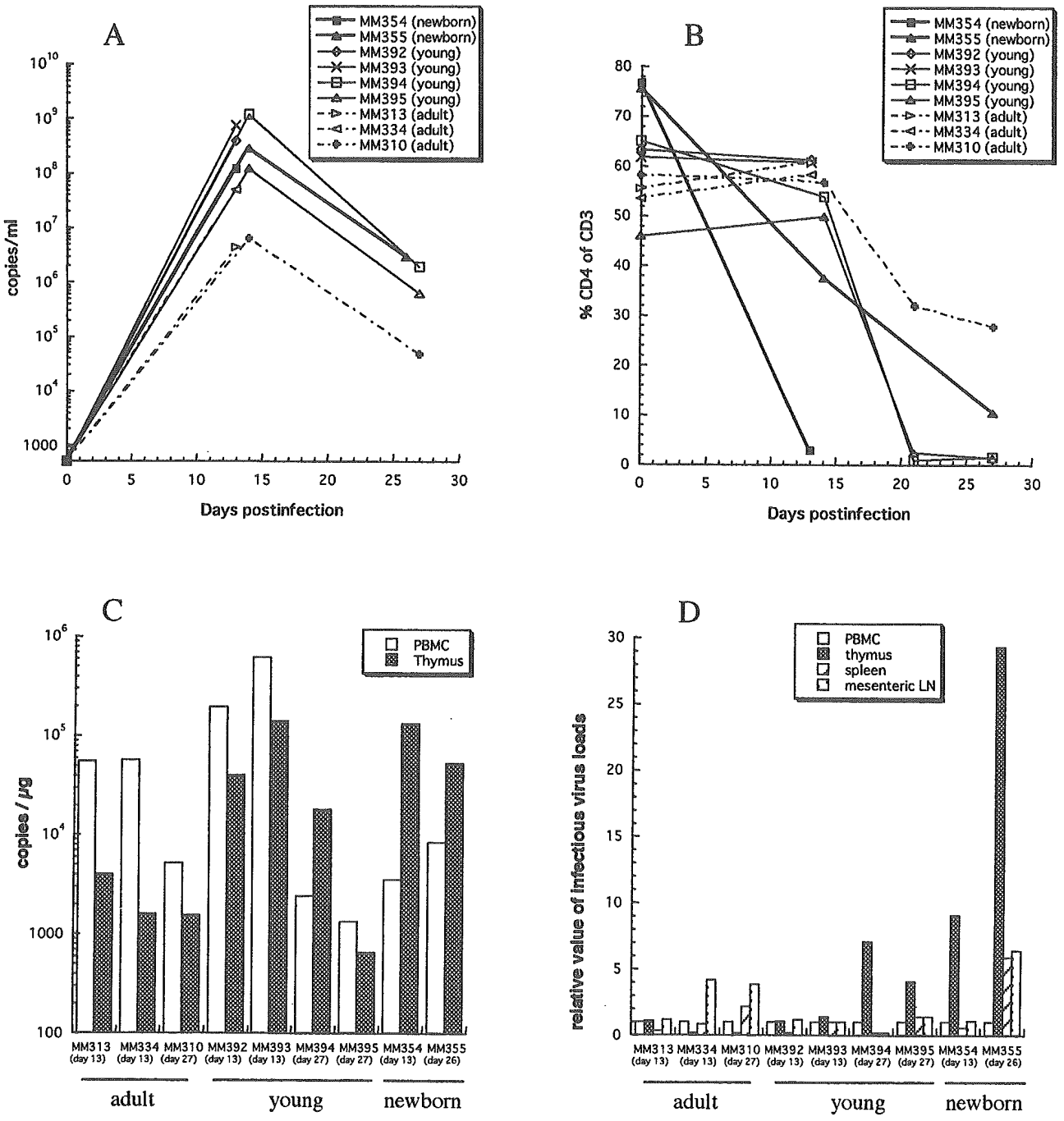

Fig. 1. Comparison of viral loads and $CD4^+$ T cell counts between newborn, young and adult macaques during acute SHIV-C2/1 infection. (A) Plasma viral RNA levels. (B) Relative frequency (percentage) of CD4 T cells. (C) Amounts of proviral DNA in PBMCs and thymus, as determined by quantitative PCR. Values are expressed as viral DNA copy numbers per microgram of total DNA extracted from single cell suspensions. (D) Infectious viral loads in lymphoid tissues relative to the viral load in PBMCs. Values were determined by infectious plaque assay.

ded in paraffin wax for histological (hematoxylin-eosin staining) and immunohistochemistry studies. Four-micrometer sections were dewaxed, pretreated by appropriate methods for each antibody (see below) and treated with TBS-Tween 20 and aqueous hydrogen peroxide. To stain CD4 antigen, sections were pretreated in 1 mM EDTA (pH 8.0) and autoclaved at 121 C for 15 min. To stain cytokeratin, sections were pretreated by proteinase K (Dako, Carpinteria, Calif., U.S.A.) at room temperature for 5 min. To stain ssDNA, sections were incubated overnight with 1% saponin at 4 C. To stain SIV-Nef antigen, sections were pretreated in 1 mM EDTA (pH 8.0) and autoclaved. Cells in the sections were stained with the following mAbs. $CD4^+$ cells were stained with anti-CD4 (NCL-CD4; Novocastra Laboratories, London, U.K.). Thymus epithelial cells were stained with anti-cytokeratin (MNF116; Dako, Carpinteria, Calif., U.S.A.). Apoptotic cells were stained with anti-ssDNA (Dako, Kyoto, Japan). Virus-positive cells were stained with anti-SIV Nef (aa 71–80; FIT Biotech Oyj Plc, Tampere, Finland) (51). Stained cells were visualized with an EnVision kit (Dako, Carpinteria, Calif., U.S.A.) and diaminobenzidine, rinsed in distilled water and counterstained with hematoxylin (Dako, Carpinteria, Calif., U.S.A.).

Results

Viral Loads and $CD4^+$ T Cells in Whole Blood

Plasma viremia of newborns reached a peak (more than 10^8 copies of RNA/ml) at 13 dpi and remained at high levels to 26 dpi. This pattern was similar to that in young and adult macaques (Fig. 1A). In all macaques, severe $CD4^+$ T cell depletion was observed within 4 weeks after inoculation (Fig. 1B). However, viral RNA levels were higher in newborn and young macaques at both 2 weeks and 4 weeks after inoculation than in adults, and were inversely correlated with $CD4^+$ T cell depletion. These data indicated that *in vivo* infectivity of acute pathogenic SHIV-C2/1 was higher in younger macaques.

The levels of proviral DNA in PBMCs and thymocytes were evaluated by performing quantitative PCR on the DNA extracted from suspensions of single cells. The proviral DNA loads in newborn thymus were highest at 13 dpi and remained at high levels to 26 dpi. In both of the infected newborns and in one of the four young macaques (MM394), the amounts of provirus were higher in thymocytes than in PBMCs. On the contrary, in all infected adults and in three of the four young macaques, the amounts of provirus were higher in PBMCs than in thymocytes (Fig. 1C). Infectious virus loads were considerably higher in thymocytes than in other lymphoid tissues in both of the infected newborns and in the two young macaques sacrificed at 27 dpi, although the amounts of infectious virus were not so different between thymocytes and other lymphoid tissues in the other infected macaques (Fig. 1D).

Alterations in the Phenotypes of Newborn Thymocytes

The profiles of lymphocyte subsets in the thymuses of the two infected newborns at 13 and 26 dpi were markedly different from the pattern observed in cells from the two uninfected controls (Table 2). As the infection period became longer, there were dramatic decreases of mature $CD3^+CD4^+CD8^-$ single positive (CD4SP) cells and immature $CD4^+CD8^+$ double positive (DP) cells and increases of immature $CD3^-CD4^-CD8^-$ triple negative (TN) cells and mature $CD3^+CD4^-CD8^+$ single positive (CD8SP) cells relative to the uninfected control. Of particular interest was the marked depletion of DP cells from about 90% to 5% and the relative increase of the percentage of TN cells from less than 1% to over 30%.

Impaired Thymopoietic Potential of $CD3^-CD4^-CD8^-$ TN Cells Due to Aging or Infection

We hypothesized that acute pathogenic SHIV infection prevents T cells from developing beyond TN cells, resulting in severe depletion of DP cells. To examine this hypothesis, we characterized the TN subsets, and evaluated the intrathymic effects of SHIV-C2/1 in more detail. The thymus is one of the most critical tissues for understanding acute pathogenicity, especially in infected newborn macaques. However, thymic function is known to be impaired with aging (1). Therefore, to better understand and to evaluate the effect of SHIV-C2/1

Table 2. Thymocyte subset changes in SHIV-C2/1-infected animals

Animal ID	% of cells				
	TN[a]	DP[b]	CD4SP[c]	CD8SP[d]	CD20
MM356 (uninfected)	0.2	90.1	7.7	1.4	<0.1
RM03 (uninfected)	0.9	86.0	9.8	1.2	0.3
MM354 (sacrificed 13 dpi)	1.1	94.2	**0.8**	1.5	<0.1
MM355 (sacrificed 26 dpi)	32.5	**5.1**	**0.9**	26.3	0.5

Values in bold represent a significant reduction and values with underbar represent a significant increase compared to uninfected controls.

[a] $CD3^-CD4^-CD8^-$ triple negative.

[b] $CD4^+CD8^+$ double positive.

[c] $CD3^+CD4^+CD8^-$ single positive.

[d] $CD3^+CD4^-CD8^+$ single positive.

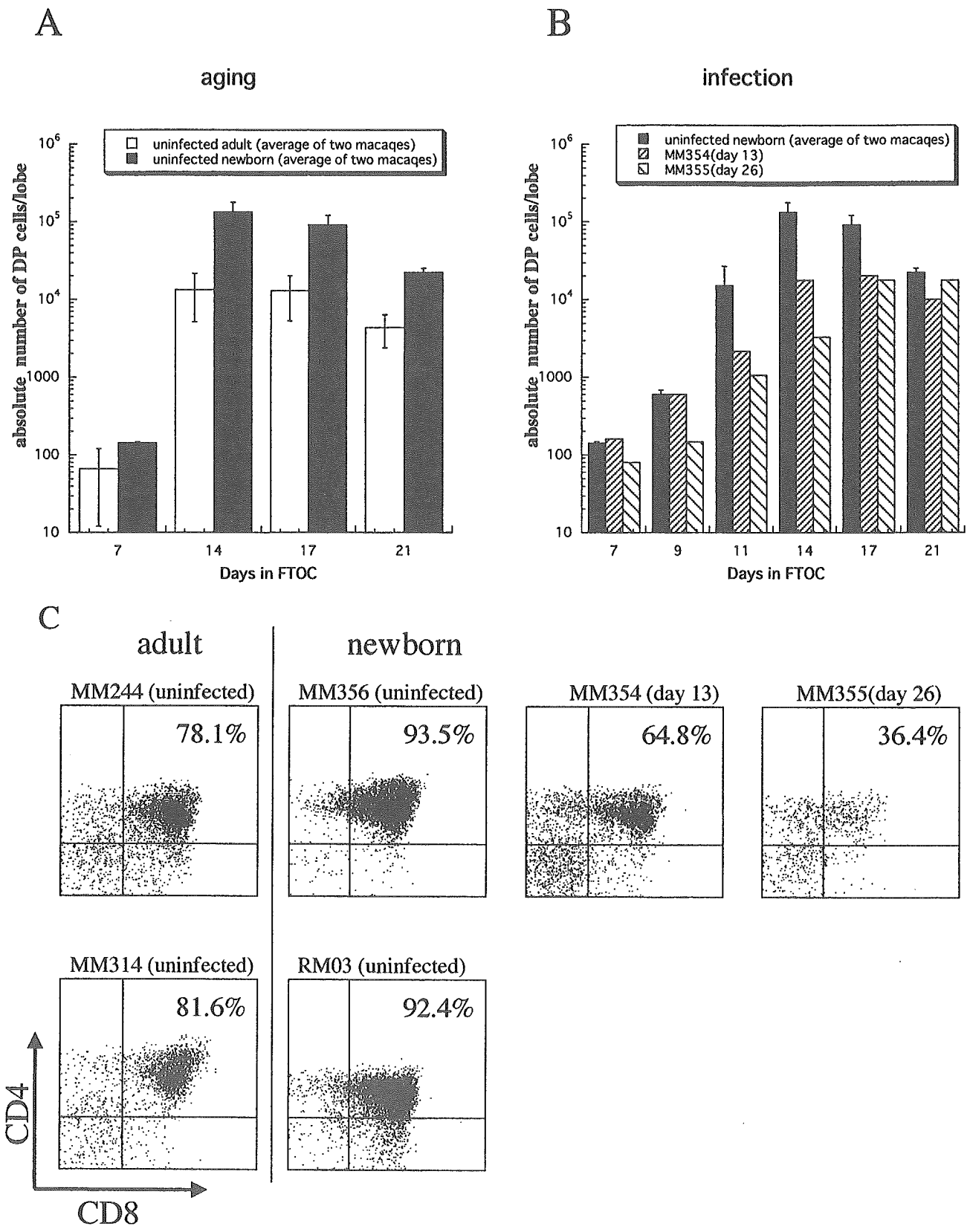

Fig. 2. Evaluation of progenitor function of $CD3^-CD4^-CD8^-$ triple negative (TN) subset in the thymus. (A) and (B) Abundance and growth kinetics of developed $CD4^+CD8^+$ double positive (DP) cells in FTOC. The absolute number of DP cells was the average cell numbers of three lobes. (A) Comparison of uninfected newborn and adult macaques to examine the effect of aging. (B) Comparison of uninfected and SHIV-C2/1-infected newborn macaques to examine the effect of infection. (C) Comparison of phenotypic maturation of TN cells into DP cells in uninfected and SHIV-C2/1-infected macaques at 14 days in FTOC.

on thymopoiesis, we must first understand the effect of normal thymic dysfunction (such as occurs as a result of aging or viral infection) on progenitor function of TN cells.

A monkey-mouse fetal thymus organ culture (FTOC) system is capable of reproducing the development of T cell progenitor from TN cells to DP cells *in vitro* (35). We evaluated the effects of aging or SHIV-C2/1 infection on T cell maturation during this period of development. The average peak absolute number of DP cells in the two uninfected adult macaques (MM244 and MM314) was about one-tenth that of uninfected newborn (MM356 and RM03). However, about 80% of the TN cells purified from uninfected adult macaques differentiated into DP cells after 14 days of FTOC (Fig. 2, A and C). In uninfected adults, 14 days of FTOC was enough to reach the peak level of differentiation, which is identical to the time required in uninfected newborns. These results suggest that thymic dysfunction by aging was due to a decrease in the number of progenitor cells that were able to develop into DP cells in the TN cells, rather than to the dysfunction that accompanies maturation of an individual progenitor.

To clarify the effect of viral infection, we compared the function of TN cells in SHIV-C2/1 infected newborns and age matched uninfected controls. The peak DP cell counts of both infected newborns (MM354 and 355) were as low as 1/7 the average of the peak DP cell counts of uninfected controls (MM356 and RM03). After 14 days of FTOC, the fractions of DP cells that differentiated from TN cells in MM354 (64.8%) and MM355 (36.4%) were lower than the fraction in uninfected newborns (over 90%). Fourteen days were required to reach the peak level of differentiation to DP cell counts in MM354 (sacrificed at 13 dpi) whereas 17 days was required to reach the peak level in MM355 (sacrificed at 26 dpi) (Fig. 2B). These data show that the effect of increasing the infection period was more to delay the differentiation than to decrease its peak level.

Phenotyping of $CD3^-CD4^-CD8^-$ TN Thymocytes

The SHIV-C2/1 infection caused a marked depletion of DP cells and a relative increase of TN cells, and impaired the thymopoietic potential of residual TN cells. We also examined the change in phenotype of TN cells. First, to evaluate the degree to which TN cells were contaminated by cells of non-T lineages, expressions of CD20 (B cells), CD11b (monocytes/macrophages), and CD16 and 56 (NK cells) were examined. Whole thymocytes from newborn macaques contained only small fractions of B cells (<1%), monocytes (<0.1%) and NK cells (<0.1%). These results indicated that the SHIV-infection did not bring about major changes to these subsets (data not shown). Second, thymocytes were stained with anti-CD2 mAb which is a marker of T cell precursors (7, 13, 52) or anti-TdT mAb which is a marker of lymphoid precursor cells (18, 29). After intrarectal infection with SHIV-

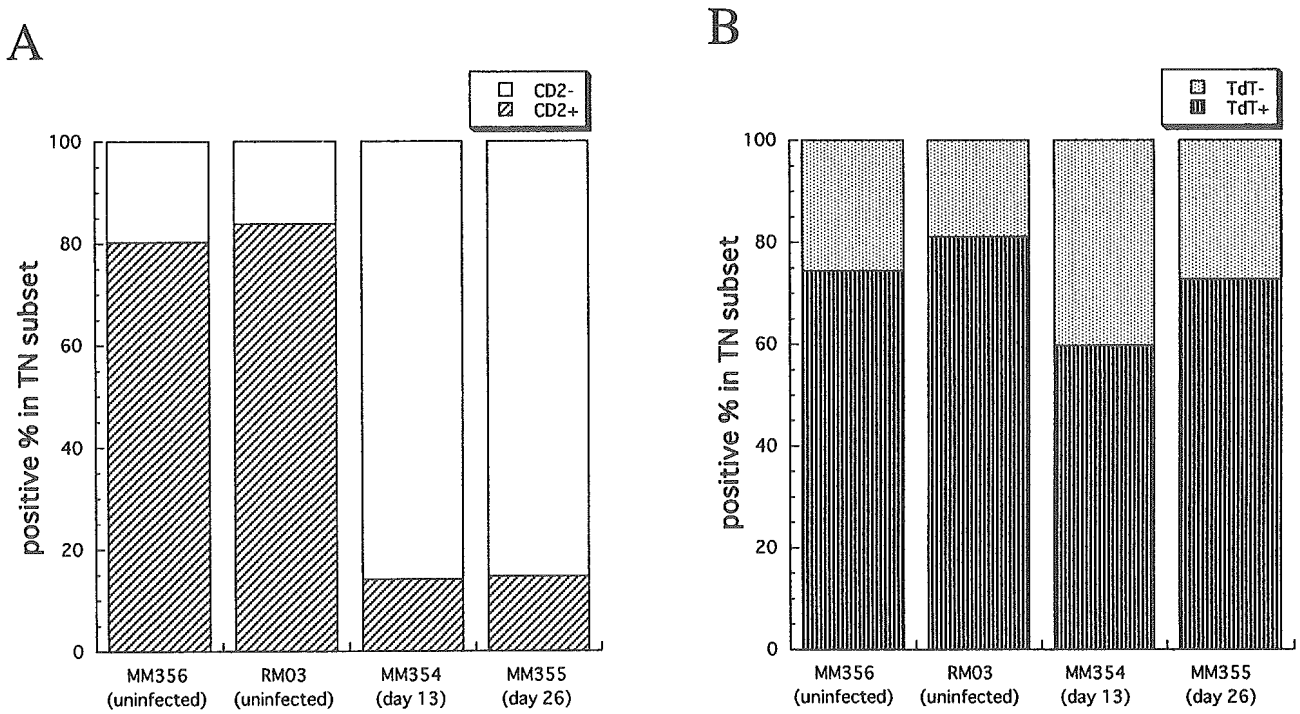

Fig. 3. Frequency of $CD2^+$ cells (A) and TdT^+ cells (B) in the TN subset during acute SHIV-C2/1 infection, as determined by flow cytometry. Thymocytes were obtained at the time of necropsy, and stained with mAbs to CD3, CD4, CD8 and CD2 or TdT.

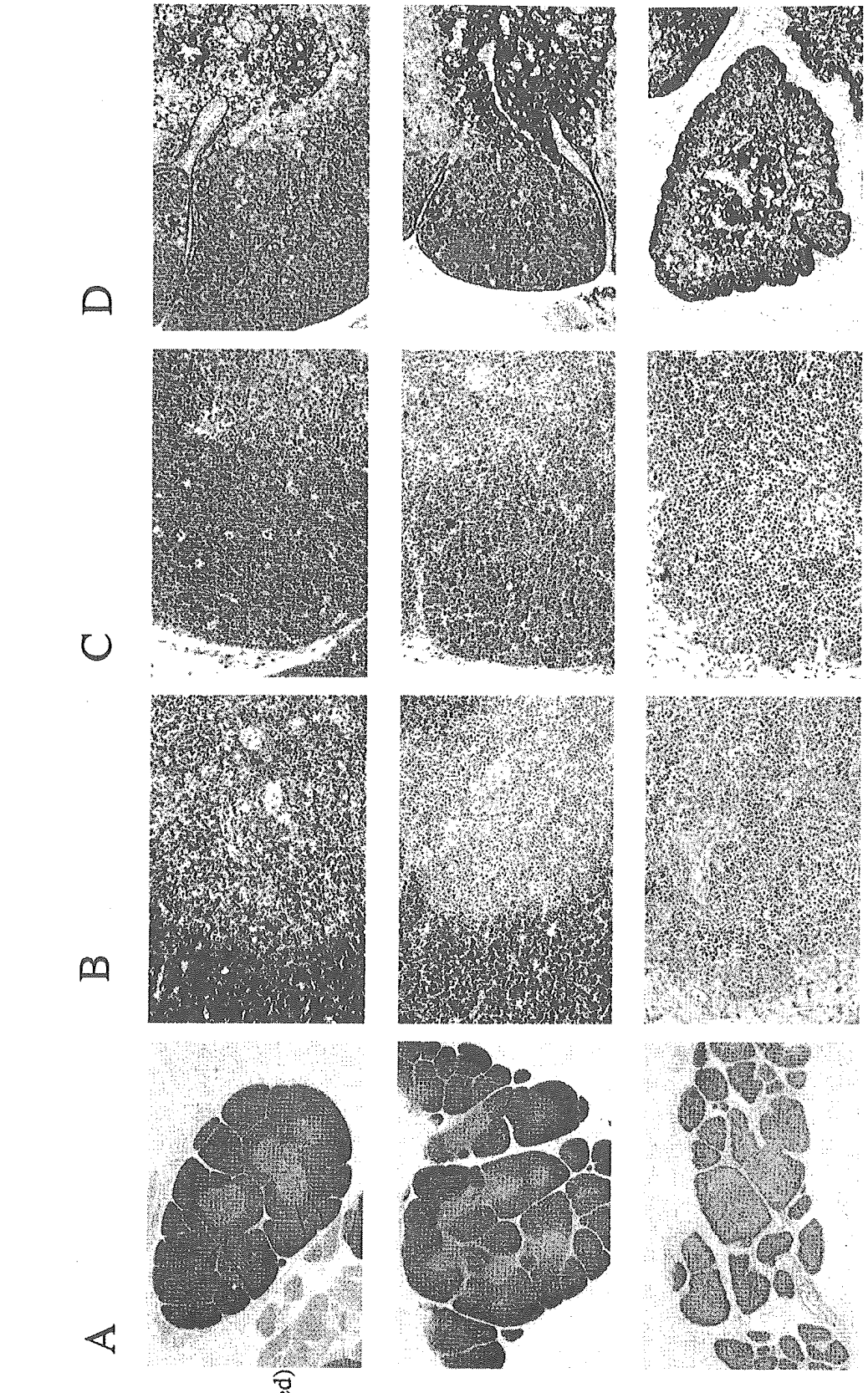

Fig. 4. Histopathological changes in thymus associated with acute SHIV-C2/1 infection. Sections of thymuses from an uninfected control macaque (MM356) as well as from newborns sacrificed at 13 dpi (MM354) and 26 dpi (MM355). Adjacent sections from the same tissue blocks were stained with (A) Hematoxylin and eosin (×40), (B) immunostained with anti-human CD4 mouse mAb (×100), (C) with single strand DNA to visualize apoptotic cells (×200) and (D) with anti-human cytokeratin mouse mAb to detect thymus epithelial cells (×100).

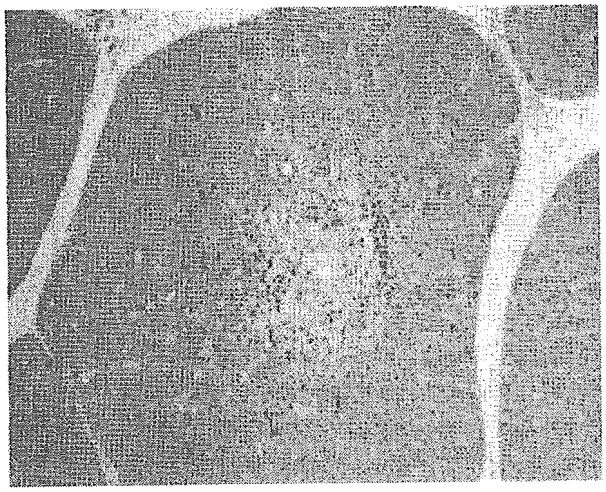

Fig. 5. Viral Nef$^+$ cells in a thymus from a newborn macaque infected with SHIV-C2/1 at 13 dpi (MM354). Thymus was immunostained with anti-SIV Nef antibody (×40).

C2/1, CD2$^+$ TN cells dramatically decreased from about 80% to 14% (Fig. 3A). By contrast, the fraction of TN cells that were TdT marker positive did not change very much after the infection (Fig. 3B).

Histopathological Analyses in the Thymus

To understand how the virus-infected thymus was altered in the early stage of infection, the SHIV-C2/1-infected thymuses were examined at 13 and 26 dpi. At 13 dpi, the thymus showed a thinning of the cortex in some lobules and mildly increased white spots like starry sky, which are tingible-body macrophages in the cortex (Fig. 4A, middle). Expansion of the medulla was observed with infiltration of neutrophilic inflammatory cells and mildly decreased density of thymocytes. The depleted cells were identified as CD4$^+$ cells by immunohistochemical examination (Fig. 4B, middle). Subsequently, the continuous progression of thymic involution resulted in small, atrophic lobules widely separated by prominent interlobular connective septa with no visible thymic cortex and no discernible corticomedullary junction at 26 dpi (Fig. 4A, bottom). The staining properties and location of apoptotic cells that were positive for single stranded DNA (DNA fragmentation) in the thymus of uninfected and infected animals are shown in Fig. 4C. At 13 dpi, apoptotic signals were increased particularly in the cortex. These signals were consistent with tingible-body macrophages which were considered in the process of phagocytosing apoptotic cells (Fig. 4C, middle). On day 26, apoptotic cells were decreased (Fig. 4C, bottom). Crosstalk between thymocytes and thymus epithelial cells is thought to be important for thymopoiesis (46). Therefore, we tested for the presence of cytokeratin-immunopositive epithelial cells. These cells were found to become more prominent in the thymus lobe with increasing infection period (Fig. 4D). These results indicate that the epithelial framework remained in the infected thymus, although acute thymic involution with severe depletion of thymocytes was observed. In the thymus of the SHIV-C2/1-infected newborn examined at 13 dpi, immunohistochemical staining showed that the majority of virus Nef$^+$ cells were located in the medulla or the corticomedullary junction, although a small number of Nef$^+$ cells were also present in the cortex (Fig. 5).

Discussion

This study demonstrated that intrarectal infection with SHIV-C2/1 caused a rapid and profound depletion of peripheral CD4$^+$ T cells in newborn rhesus macaques, as was previously observed to occur in young and adult macaques. However, in newborn macaques, viral loads in the thymus were much higher than those in other tissues, whereas no clear difference of viral loads was observed among lymphoid tissues in adults, and intermediate results were observed in young macaques (Fig. 1, C and D). These results indicate that the distribution of virus in different tissues in the newborns early after mucosal infection was considerably different from that in adults. Since membrane fluidity influences the HIV-1 infectivity (9, 10), it may be interesting to determine the plasma membrane fluidity of infant thymocytes.

We employed a monkey-mouse FTOC system to evaluate the progenitor function of TN cells. This assay can directly measure thymopoiesis in the immature stage. TN cells isolated from newborns produced more CD4-expressing cells in FTOC than did TN cells isolated from adults (Fig. 2A). That is, the thymus of newborns can supply a greater number of virus target cells than can the thymus of adults. Taken together, these findings suggest that the thymus is a major site of viral replication and an important target organ in the pathogenicity of AIDS in newborns. Table 2 shows that severe DP cell depletion occurred at 26 dpi. This result and the histological results are similar to what was observed in a newborn human with congenital HIV-1 infection (44). The thymus of this individual showed severe depletion of both CD4 single positive and DP subsets.

In previously studied SIV infections, the depletion of DP cells was temporary (between 14 and 21 days). In contrast, the depletion of DP cells was stable in SHIV-infected monkeys, although there was an increase of apoptotic thymocytes coincident with the peak of SIV-viremia similar to SHIV-infected monkeys (45). This

difference suggest that some mechanism other than direct killing and apoptosis is responsible for the depletion of DP cells. A recent study demonstrated that HIV infection caused a rapid and sustained suppression of thymocyte proliferation (5). This study used an indirect assay in PBMCs, based on the ratio of different T cell receptor excision circles, which are molecular markers of distinct T cell rearrangements occurring at different stages of T cell development. In the present study, we directly measured thymopoiesis using the FTOC system, and showed that SHIV-C2/1 infection impaired progenitor function of the thymocytes. The impairment was of the progenitor itself, and not due to the destruction of the thymic environment that is indispensable to thymopoiesis, because the xenogeneic FTOC used mouse stroma that are non-sensitive to SHIV infection.

MM354 (at 13 dpi) showed considerable depletion of mature CD4 single positive cells (Table 2) and mild thymic atrophy with $CD4^+$ cell depletion in the medulla (Fig. 4, A and B, middle panels). Most of the virus-infected cells were localized in this area (Fig. 5). At the same time in the FTOC, the ability of TN cells in the thymus to differentiate to DP cells was already impaired (Fig. 2B), although the FACS analysis detected no appreciable change in DP subsets in the thymus (Table 2). At 26 dpi (MM355), DP cells were severely depleted (Table 2) and the cortex region in the thymus disappeared (Fig. 4A, bottom panel). Immature thymocytes are mainly present in the cortex, whereas mature thymocytes are mainly present in the medulla (2). That is, an impaired thymopoiesis measured by FTOC is predictive of DP cell depletion in the thymus *in vivo*. Taken together, these results indicate that the early stage of infection in newborn macaques infected intrarectally with SHIV-C2/1 has two phases. The first phase is direct infection and active replication in mature $CD4^+$ cells that result in the depletion of mature CD4 single positive cells in the thymus that was observed at 13 dpi. The thymus in this phase is probably the main source of the virus production causing the peak of plasma viremia. The second phase, which was observed at 26 dpi, after the peak of plasma viremia, is the immature cell depletion phase and was caused by the impairment of thymopoiesis. These data also indicate that SHIV-C2/1 infection affects immature thymocytes, especially as the infection period became longer.

In this study, we showed impaired thymopoietic potential of TN cells from acute SHIV-C2/1-infected macaques. Neben et al. showed that the thymopoietic potential of $CD3^-CD4^+CD8^-$ cells, but not TN cells, was impaired in the acute phase of SIV infection (35). *De novo* generation of naïve T cells occurs in the thymus after progenitors migrate from bone marrow. These progenitor cells differentiate from TN into $CD3^-CD4^+CD8^-$ cells and in the next step into DP cells. That is, SHIV-C2/1 infection affects T cell development in the thymus at earlier stage than does SIV infection *in vivo*. We previously observed a greater number of virus-expressing cells in thymuses infected with acute pathogenic SHIV than in thymuses infected with SIV at the early stage of intravenous infection (48). A histopathological study of pathogenic SHIV-infected thymus showed differences in thymic pathology based on coreceptor usage controlled by the HIV-1 env gene. The thymic atrophy associated with X4-utilizing SHIV was more severe than that of R5-utilizing SHIV (42). The thymus of the newborn examined at 26 days after infection with SHIV-C2/1 (which uses X4 in addition to R5) showed severe thymic atrophy with depletion of cortical cells. Similar symptoms were observed in an infant monkey infected with an X4-utilizing SHIV (42). SIV generally uses R5 rather than X4 as a coreceptor. Taken together, these results suggest that utilization of X4 as the coreceptor is highly associated with the thymus tropism and that the virus burden in the thymus is the key factor impairing the progenitor function of TN cells *in vivo*.

Both infected newborn macaques showed a reduced number of differentiated DP cells in FTOC compared with the uninfected controls (Fig. 2B). While determining the culture conditions for the FTOC, we noticed that if we used less than the normal number of cells (2,000) in the uninfected control experiment, the peak levels of differentiated DP cell counts were reduced, although the time to reach the peak was the same as it was when 2,000 cells were used (14 days) (data not shown). Since the time to reach the peak level of DP cell counts of MM354 (14 days) was the same as that in the uninfected controls, the impairment of thymopoiesis as a result of SHIV-C2/1 infection at 13 dpi could be attributed to the quantitative decrease of the subpopulation of TN cells that are able to differentiate to DP cells in FTOC. On the other hand, MM355 took more time (17 days) to reach the peak, although the peak level of DP cell counts was almost the same as that in MM354. This result suggests that the proliferation ability of TN cells at 26 dpi is impaired by poor functioning of the cells. This impairment is in addition to the impairment at 13 dpi, which is mostly due to a decrease in the number of functional progenitor cells. FACS analysis of the TN cell population showed selective reduction of $CD2^+$ TN subsets (Fig. 3A). The sequence of development of thymocytes is $CD2^-TN \rightarrow CD2^+TN \rightarrow CD3^-CD4^+CD8^- \rightarrow DP$ in the early stages of thymic T-cell ontogeny (8, 25). Taken together, these data suggest that the $CD2^+TN$ subset is

the main population of TN cells that can develop to DP cells in FTOC.

In conclusion, the thymus appears to be the major site of viral replication and amplification in newborn macaques infected with SHIV-C2/1. As a result of SHIV-C2/1 infection, T-cell progenitors in the thymus were impaired and the $CD2^+$TN subpopulation was selectively decreased. Moreover, our findings revealed a substantial reduction of proliferation and impaired maturation of TN cells after peak viremia and the onset of CD4 depletion. However, additional studies are needed to clarify the mechanism by which thymopoiesis is impaired. Our results provide experimental evidence that an X4-utilizing acute pathogenic SHIV infection induced severe thymic atrophy and impairment of thymopoiesis in the early stage of infection. They also provide the basis for a pathogenic model, in which impaired thymopoiesis leads to profound and irreversible peripheral $CD4^+$ T cell depletion. In HIV-1-infected children, there are markers of thymic dysfunction that can predict survival outcome. Mathematical models have suggested that thymic dysinvolution in children is more severe than it is in adults, particularly in X4 virus infections (24, 54). Thus, SHIV-C2/1 infection in newborn macaques can be a useful model of HIV-1-infected children that have a rapid course of disease progression.

We thank James Raymond for English editing of this manuscript. We are grateful to Takahito Kazama and Ai Himeno for technical assistance and to Dako Corporation for technical support. This work was supported by a Health Sciences Research Grant from the Ministry of Health, Labour and Welfare, Japan, a Grant-in-Aid for Scientific Research from the Ministry of Education, Culture, Sports, Science and Technology, Japan and a Research Grant on Health Sciences focusing on Drug Innovation from the Japan Health Sciences Foundation. HS was supported by the 21st Century COE Program of the Ministry of Education, Culture, Sports, Science and Technology, Japan.

References

1) Aspinall, R., and Andrew, D. 2000. Thymic involution in aging. J. Clin. Immunol. **20**: 250–256.
2) Berzins, S.P., Uldrich, A.P., Sutherland, J.S., Gill, J., Miller, J.F., Godfrey, D.I., and Boyd, R.L. 2002. Thymic regeneration: teaching an old immune system new tricks. Trends Mol. Med. **8**: 469–476.
3) Blanche, S., Tardieu, M., Duliege, A., Rouzioux, C., Le Deist, F., Fukunaga, K., Caniglia, M., Jacomet, C., Messiah, A., and Griscelli, C. 1990. Longitudinal study of 94 symptomatic infants with perinatally acquired human immunodeficiency virus infection. Evidence for a bimodal expression of clinical and biological symptoms. Am. J. Dis. Child. **144**: 1210–1215.
4) Connor, R.I., Sheridan, K.E., Ceradini, D., Choe, S., and Landau, N.R. 1997. Change in coreceptor use correlates with disease progression in HIV-1-infected individuals. J. Exp. Med. **185**: 621–628.
5) Dion, M.L., Poulin, J.F., Bordi, R., Sylvestre, M., Corsini, R., Kettaf, N., Dalloul, A., Boulassel, M.R., Debre, P., Routy, J.P., Grossman, Z., Sekaly, R.P., and Cheynier, R. 2004. HIV infection rapidly induces and maintains a substantial suppression of thymocyte proliferation. Immunity **21**: 757–768.
6) Douek, D.C., Betts, M.R., Hill, B.J., Little, S.J., Lempicki, R., Metcalf, J.A., Casazza, J., Yoder, C., Adelsberger, J.W., Stevens, R.A., Baseler, M.W., Keiser, P., Richman, D.D., Davey, R.T., and Koup, R.A. 2001. Evidence for increased T cell turnover and decreased thymic output in HIV infection. J. Immunol. **167**: 6663–6668.
7) Gaulton, G.N., Scobie, J.V., and Rosenzweig, M. 1997. HIV-1 and the thymus. AIDS **11**: 403–414.
8) Gore, S.D., Kastan, M.B., and Civin, C.I. 1991. Normal human bone marrow precursors that express terminal deoxynucleotidyl transferase include T-cell precursors and possible lymphoid stem cells. Blood **77**: 1681–1690.
9) Harada, S., Akaike, T., Yusa, K., and Maeda, Y. 2004. Adsorption and infectivity of human immunodeficiency virus type 1 are modified by the fluidity of the plasma membrane for multiple-site binding. Microbiol. Immunol. **48**: 347–355.
10) Harada, S., Yusa, K., and Maeda, Y. 2004. Heterogeneity of envelope molecules shown by different sensitivities to anti-V3 neutralizing antibody and CXCR4 antagonist regulates the formation of multiple-site binding of HIV-1. Microbiol. Immunol. **48**: 357–365.
11) Hattori, N., Kawamoto, H., and Katsura, Y. 1996. Isolation of the most immature population of murine fetal thymocytes that includes progenitors capable of generating T, B, and myeloid cells. J. Exp. Med. **184**: 1901–1908.
12) Hatzakis, A., Touloumi, G., Karanicolas, R., Karafoulidou, A., Mandalaki, T., Anastassopoulou, C., Zhang, L., Goedert, J.J., Ho, D.D., and Kostrikis, L.G. 2000. Effect of recent thymic emigrants on progression of HIV-1 disease. Lancet **355**: 599–604.
13) Haynes, B.F., Denning, S.M., Singer, K.H., and Kurtzberg, J. 1989. Ontogeny of T-cell precursors: a model for the initial stages of human T-cell development. Immunol. Today **10**: 87–91.
14) Haynes, B.F., Hale, L.P., Weinhold, K.J., Patel, D.D., Liao, H.X., Bressler, P.B., Jones, D.M., Demarest, J.F., Gebhard-Mitchell, K., Haase, A.T., and Bartlett, J.A. 1999. Analysis of the adult thymus in reconstitution of T lymphocytes in HIV-1 infection. J. Clin. Invest. **103**: 921.
15) Igarashi, T., Endo, Y., Englund, G., Sadjadpour, R., Matano, T., Buckler, C., Buckler-White, A., Plishka, R., Theodore, T., Shibata, R., and Martin, M. 1999. Emergence of a highly pathogenic simian/human immunodeficiency virus in a rhesus macaque treated with anti-CD8 mAb during a primary infection with a nonpathogenic virus. Proc. Natl. Acad. Sci. U.S.A. **96**: 14049–14054.
16) Igarashi, T., Brown, C.R., Byrum, R.A., Nishimura, Y., Endo, Y., Plishka, R.J., Buckler, C., Buckler-White, A.,

Miller, G., Hirsch, V.M., and Martin, M.A. 2002. Rapid and irreversible CD4+ T-cell depletion induced by the highly pathogenic simian/human immunodeficiency virus SHIV (DH12R) is systemic and synchronous. J. Virol. **76**: 379–391.

17) Iida, T., Ichimura, H., Shimada, T., Ibuki, K., Ui, M., Tamaru, K., Kuwata, T., Yonehara, S., Imanishi, J., and Hayami, M. 2000. Role of apoptosis induction in both peripheral lymph nodes and thymus in progressive loss of CD4+cells in SHIV-infected macaques. AIDS Res Hum. Retroviruses **16**: 9–18.
18) Ismaili, J., Antica, M., and Wu, L. 1996. CD4 and CD8 expression and T cell antigen receptor gene rearrangement in early intrathymic precursor cells. Eur. J. Immunol. **26**: 731–737.
19) Jensen, M.A., and van't Wout, A.B. 2003. Predicting HIV-1 coreceptor usage with sequence analysis. AIDS Rev. **5**: 104–112.
20) Joag, S.V., Li, Z., Foresman, L., Stephens, E.B., Zhao, L.J., Adany, I., Pinson, D.M., McClure, H.M., and Narayan, O. 1996. Chimeric simian/human immunodeficiency virus that causes progressive loss of CD4+ T cells and AIDS in pig-tailed macaques. J. Virol. **70**: 3189–3197.
21) Joag, S.V., Li, Z., Wang, C., Jia, F., Foresman, L., Adany, I., Pinson, D.M., Stephens, E.B., and Narayan, O. 1998. Chimeric SHIV that causes CD4+ T cell loss and AIDS in rhesus macaques. J. Med. Primatol. **27**: 59–64.
22) Joshi, V.V., Oleske, J.M., Saad, S., Gadol, C., Connor, E., Bobila, R., and Minnefor, A.B. 1986. Thymus biopsy in children with acquired immunodeficiency syndrome. Arch. Pathol. Lab. Med. **110**: 837–842.
23) Kawamoto, H., Ohmura, K., Hattori, N., and Katsura, Y. 1997. Hemopoietic progenitors in the murine fetal liver capable of rapidly generating T cells. J. Immunol. **158**: 3118–3124.
24) Kirschner, D.E., Mehr, R., and Perelson, A.S. 1998. Role of the thymus in pediatric HIV-1 infection. J. Acquir. Immune Defic. Syndr. Hum. Retrovirol. **18**: 95–109.
25) Knoules, D.M., Chadburn, A., and Inghirami, G. 1992. Immunophenotypic markers useful in the diagnosis and classification of hematopoietic neoplasms, p. 73–167. *In* Knoules, D.M. (ed), Neoplastic hematopathology, Williams & Wilkins, Baltimore.
26) Kourtis, A.P., Ibegbu, C.C., Scinicariello, F., Oh, C.Y., and McClure, H.M. 2002. SHIV-KB9 infection of rhesus monkeys does not always cause disease-contribution of host immune factors and thymic output. Virology **303**: 47–57.
27) Kozyrev, I.L., Ibuki, K., Shimada, T., Kuwata, T., Takemura, T., Hayami, M., and Miura, T. 2001. Characterization of less pathogenic infectious molecular clones derived from acute-pathogenic SHIV-89.6P stock virus. Virology **282**: 6–13.
28) Kuwata, T., Igarashi, T., Ido, E., Jin, M., Mizuno, A., Chen, J. and Hayami, M. 1995. Construction of human immunodeficiency virus 1/simian immunodeficiency virus strain mac chimeric viruses having vpr and/or nef of different parental origins and their *in vitro* and *in vivo* replication. J. Gen. Virol. **76** (Pt 9): 2181−2191.
29) Lau, L.G., Tan, L.K., Koay, E.S., Ee, M.H., Tan, S.H., and Liu, T.C. 2004. Acute lymphoblastic leukemia with the phenotype of a putative B-cell/T-cell bipotential precursor. Am. J. Hematol. **77**: 156–160.
30) Madea, B., Roewert, H.J., Krueger, G.R., Ablashi, D.V., and Josephs, S.F. 1990. Search for early lesions following human immunodeficiency virus type 1 infection. A study of six individuals who died a violent death after seroconversion. Arch. Pathol. Lab. Med. **114**: 379–382.
31) Meyers, A., Shah, A., Cleveland, R.H., Cranley, W.R., Wood, B., Sunkle, S., Husak, S., and Cooper, E.R. 2001. Thymic size on chest radiograph and rapid disease progression in human immunodeficiency virus 1-infected children. Pediatr. Infect. Dis. J. **20**: 1112–1118.
32) Miyake, A., Akagi, T., Enose, Y., Ueno, M., Kawamura, M., Horiuchi, R., Hiraishi, K., Adachi, M., Serizawa, T., Narayan, O., Akashi, M., Baba, M., and Hayami, M. 2004. Induction of HIV-specific antibody response and protection against vaginal SHIV transmission by intranasal immunization with inactivated SHIV-capturing nanospheres in macaques. J. Med. Virol. **73**: 368–377.
33) Miyake, A., Enose, Y., Ohkura, S., Suzuki, H., Kuwata, T., Shimada, T., Kato, S., Narayan, O., and Hayami, M. 2004. The quantity and diversity of infectious viruses in various tissues of SHIV-infected monkeys at the early and AIDS stages. Arch. Virol. **149**: 943–955.
34) Nahmias, A.J., Clark, W.S., Kourtis, A.P., Lee, F.K., Cotsonis, G., Ibegbu, C., Thea, D., Palumbo, P., Vink, P., Simonds, R.J., and Nesheim, S.R. 1998. Thymic dysfunction and time of infection predict mortality in human immunodeficiency virus-infected infants. CDC perinatal AIDS collaborative transmission study group. J. Infect. Dis. **178**: 680–685.
35) Neben, K., Heidbreder, M., Muller, J., Marxer, A., Petry, H., Didier, A., Schimpl, A., Hunig, T., and Kerkau, T. 1999. Impaired thymopoietic potential of immature CD3(−) CD4(+)CD8(−) T cell precursors from SIV-infected rhesus monkeys. Int. Immunol. **11**: 1509–1518.
36) Nishimura, Y., Igarashi, T., Donau, O.K., Buckler-White, A., Buckler, C., Lafont, B.A., Goeken, R.M., Goldstein, S., Hirsch, V.M., and Martin, M.A. 2004. Highly pathogenic SHIVs and SIVs target different CD4+ T cell subsets in rhesus monkeys, explaining their divergent clinical courses. Proc. Natl. Acad. Sci. U.S.A. **101**: 12324–12329.
37) Papiernik, M., Brossard, Y., Mulliez, N., Roume, J., Brechot, C., Barin, F., Goudeau, A., Bach, J.F., Griscelli, C., Henrion, R., et al. 1992. Thymic abnormalities in fetuses aborted from human immunodeficiency virus type 1 seropositive women. Pediatrics **89**: 297–301.
38) Penn, M.L., Grivel, J.C., Schramm, B., Goldsmith, M.A., and Margolis, L. 1999. CXCR4 utilization is sufficient to trigger CD4+ T cell depletion in HIV-1-infected human lymphoid tissue. Proc. Natl. Acad. Sci. U.S.A. **96**: 663–668.
39) Picker, L.J., Hagen, S.I., Lum, R., Reed-Inderbitzin, E.F., Daly, L.M., Sylwester, A.W., Walker, J.M., Siess, D.C., Piatak, M., Jr., Wang, C., Allison, D.B., Maino, V.C., Lifson, J.D., Kodama, T., and Axthelm, M.K. 2004. Insufficient production and tissue delivery of CD4+ memory T cells in rapidly progressive simian immunodeficiency virus

infection. J. Exp. Med. **200**: 1299–1314.
40) Prevot, S., Audouin, J., Andre-Bougaran, J., Griffais, R., Le Tourneau, A., Fournier, J.G., and Diebold, J. 1992. Thymic pseudotumorous enlargement due to follicular hyperplasia in a human immunodeficiency virus sero-positive patient. Immunohistochemical and molecular biological study of viral infected cells. Am. J. Clin. Pathol. **97**: 420–425.
41) Reimann, K.A., Li, J.T., Veazey, R., Halloran, M., Park, I.W., Karlsson, G.B., Sodroski, J., and Letvin, N.L. 1996. A chimeric simian/human immunodeficiency virus expressing a primary patient human immunodeficiency virus type 1 isolate env causes an AIDS-like disease after *in vivo* passage in rhesus monkeys. J. Virol. **70**: 6922–6928.
42) Reyes, R.A., Canfield, D.R., Esser, U., Adamson, L.A., Brown, C.R., Cheng-Mayer, C., Gardner, M.B., Harouse, J.M., and Luciw, P.A. 2004. Induction of simian AIDS in infant rhesus macaques infected with CCR5- or CXCR4-utilizing simian-human immunodeficiency viruses is associated with distinct lesions of the thymus. J. Virol. **78**: 2121–2130.
43) Richardson, M.W., Sverstiuk, A., Hendel, H., Cheung, T.W., Zagury, J.F., and Rappaport, J. 2000. Analysis of telomere length and thymic output in fast and slow/non-progressors with HIV infection. Biomed. Pharmacother. **54**: 21–31.
44) Rosenzweig, M., Clark, D.P., and Gaulton, G.N. 1993. Selective thymocyte depletion in neonatal HIV-1 thymic infection. AIDS **7**: 1601–1605.
45) Rosenzweig, M., Connole, M., Forand-Barabasz, A., Tremblay, M.P., Johnson, R.P., and Lackner, A.A. 2000. Mechanisms associated with thymocyte apoptosis induced by simian immunodeficiency virus. J. Immunol. **165**: 3461–3468.
46) Rothe, M., Chene, L., Nugeyre, M.T., Braun, J., Barre-Sinoussi, F., and Israel, N. 1998. Contact with thymic epithelial cells as a prerequisite for cytokine-enhanced human immunodeficiency virus type 1 replication in thymocytes. J. Virol. **72**: 5852–5861.
47) Shibata, R., Maldarelli, F., Siemon, C., Matano, T., Parta, M., Miller, G., Fredrickson, T., and Martin, M.A. 1997. Infection and pathogenicity of chimeric simian-human immunodeficiency viruses in macaques: determinants of high virus loads and CD4 cell killing. J. Infect. Dis. **176**: 362–373.
48) Shimada, T., Suzuki, H., Motohara, M., Kuwata, T., Ibuki, K., Ui, M., Iida, T., Fukumoto, M., Miura, T., and Hayami, M. 2003. Comparative histopathological studies in the early stages of acute pathogenic and nonpathogenic SHIV-infected lymphoid organs. Virology **306**: 334–346.
49) Shinohara, K., Sakai, K., Ando, S., Ami, Y., Yoshino, N., Takahashi, E., Someya, K., Suzaki, Y., Nakasone, T., Sasaki, Y., Kaizu, M., Lu, Y., and Honda, M. 1999. A highly pathogenic simian/human immunodeficiency virus with genetic changes in cynomolgus monkey. J. Gen. Virol **80** (Pt 5): 1231−1240.
50) Su, L., Kaneshima, H., Bonyhadi, M.L., Lee, R., Auten, J., Wolf, A., Du, B., Rabin, L., Hahn, B.H., Terwilliger, E., and McCune, J.M. 1997. Identification of HIV-1 determinants for replication *in vivo*. Virology **227**: 45–52.
51) Sugimoto, C., Tadakuma, K., Otani, I., Moritoyo, T., Akari, H., Ono, F., Yoshikawa, Y., Sata, T., Izumo, S., and Mori, K. 2003. Nef gene is required for robust productive infection by simian immunodeficiency virus of T-cell-rich paracortex in lymph nodes. J. Virol. **77**: 4169–4180.
52) Terstappen, L.W., Huang, S., and Picker, L.J. 1992. Flow cytometric assessment of human T-cell differentiation in thymus and bone marrow. Blood **79**: 666–677.
53) Watanabe, Y., and Katsura, Y. 1993. Development of T cell receptor alpha beta-bearing T cells in the submersion organ culture of murine fetal thymus at high oxygen concentration. Eur. J. Immunol. **23**: 200–205.
54) Ye, P., Kourtis, A.P., and Kirschner, D.E. 2002. The effects of different HIV type 1 strains on human thymic function. AIDS Res. Hum. Retroviruses **18**: 1239–1251.
55) Zhang, Y., Lou, B., Lal, R.B., Gettie, A., Marx, P.A., and Moore, J.P. 2000. Use of inhibitors to evaluate coreceptor usage by simian and simian/human immunodeficiency viruses and human immunodeficiency virus type 2 in primary cells. J. Virol. **74**: 6893–6910.

Available online at www.sciencedirect.com
SCIENCE DIRECT®
ELSEVIER
Virology 343 (2005) 151 – 161
VIROLOGY
www.elsevier.com/locate/yvir

Induction of immune response in macaque monkeys infected with simian–human immunodeficiency virus having the TNF-α gene at an early stage of infection

Yuya Shimizu [a], Yasuyuki Miyazaki [b], Kentaro Ibuki [b], Hajime Suzuki [b], Kentaro Kaneyasu [b], Yoshitaka Goto [a], Masanori Hayami [b], Tomoyuki Miura [b], Takeshi Haga [a,*]

[a] *Department of Veterinary Microbiology, University of Miyazaki, Miyazaki 889-2192, Japan*
[b] *Laboratory of Primate Model, Experimental Research Center for Infectious Disease, Institute for Virus Research, Kyoto University, Kyoto 606-8507, Japan*

Received 23 April 2005; returned to author for revision 7 June 2005; accepted 18 August 2005
Available online 16 September 2005

Abstract

TNF-α has been implicated in the pathogenesis of, and the immune response against, HIV-1 infection. To clarify the roles of TNF-α against HIV-1-related virus infection in an SHIV-macaque model, we genetically engineered an SHIV to express the TNF-α gene (SHIV-TNF) and characterized the virus's properties in vivo. After the acute viremic stage, the plasma viral loads declined earlier in the SHIV-TNF-inoculated monkeys than in the parental SHIV (SHIV-NI)-inoculated monkeys. SHIV-TNF induced cell death in the lymph nodes without depletion of circulating $CD4^+$ T cells. SHIV-TNF provided some immunity in monkeys by increasing the production of the chemokine RANTES and by inducing an antigen-specific proliferation of lymphocytes. The monkeys immunized with SHIV-TNF were partly protected against a pathogenic SHIV (SHIV-C2/1) challenge. These findings suggest that TNF-α contributes to the induction of an effective immune response against HIV-1 rather than to the progression of disease at the early stage of infection.

Keywords: SHIV; TNF-α; Immune response; Cytokines; Proliferation; RANTES; HIV-1; SIV

Introduction

Cytokines mediate important immunoregulatory functions, and changes in their relative levels play key roles in the immune response against human immunodeficiency virus type-1 (HIV-1) infection and the progression of HIV-1 infection to clinical AIDS (Fauci, 1996; Matsuyama et al., 1991). Increased levels of proinflammatory cytokines, especially tumor necrosis factor alpha (TNF-α) and interleukin-6 (IL-6), were detected in plasma and tissue of patient with AIDS (Fauci, 1993; Navikas et al., 1995). TNF-α has been strongly implicated in the progression of HIV-1 infection (Aukrust et al., 1994). A possible mechanism for the progression of HIV-1 infection is that TNF-α enhances HIV-1 replication (Folks et al., 1989; Poli et al., 1990). Another possibility is that TNF-α induces apoptosis of lymphocytes (Zheng et al., 1995), which destroys T cells in the peripheral lymphoid systems (Badley et al., 1997; Herbein et al., 1998).

On the other hand, TNF-α is also involved in controlling the immune responses in some viral infections (Herbein and O'Brien, 2000). Pretreatment of TNF-α inhibited replication of the monocyte-tropic strain of HIV-1 (Herbein and Gordon, 1997). Thus, as a pleiotropic cytokine, TNF-α might contribute not only to the pathogenesis of HIV-1 infection but also to the immune response against HIV-1 infection. Despite the importance of TNF-α, little information is available on its role in the pathogenesis of HIV-1 infection in vivo. The early events of infection are especially unclear because it is difficult to monitor humans immediately after they are infected.

Chimeric simian and human immunodeficiency virus (SHIV) clones containing the HIV-1 *tat*, *rev*, *vpu*, and *env* genes on a simian immunodeficiency virus (SIV) strain mac239 background readily infected several susceptible macaques. Inoculation of macaque monkeys with SHIV is an

* Corresponding author. Fax: +81 985 58 7575.
E-mail address: a0d518u@cc.miyazaki-u.ac.jp (T. Haga).

0042-6822/$ - see front matter © 2005 Elsevier Inc. All rights reserved.
doi:10.1016/j.virol.2005.08.025

important tool for studying the early stage of an HIV-1-like infection, for elucidating the etiology of AIDS, and for evaluating the protective effects of vaccine candidates in vivo. We previously reported the in vivo properties of one of the SHIVs, SHIV-NM3rN (Kuwata et al., 1995). To assess the role of cytokines in the pathogenesis of HIV-1-related virus infection, the SHIV-*nef* vector having unique restriction enzyme sites (designated as SHIV-NI) was constructed from SHIV-NM3rN. Gene-deleted SHIVs can serve as vectors that express cytokine genes in infected macaque monkeys (Enose et al., 2004; Kozyrev et al., 2002). SHIV vectors containing a cytokine gene appear to be appropriate tools for observing the role of local production of a cytokine on virus replication, pathogenesis, and immunogenicity, especially because the inserted cytokine gene is expressed in the region where the SHIV vector replicates.

To study the role of TNF-α against HIV-1-related virus infection in an SHIV-macaque model, we constructed an SHIV in which the *nef* gene is replaced with a human TNF-α coding sequence (SHIV-TNF). In a previous in vitro study (Haga et al., 2002), we showed that SHIV-TNF (i) expressed a significant amount of biologically active TNF-α, (ii) replicated better than the parental SHIV-NI in monkey peripheral blood mononuclear cells (PBMCs), and (iii) induced a more severe cell death in monkey PBMCs than did the parental SHIV-NI.

In this study, we demonstrate that inoculation of SHIV-TNF in macaque monkeys induced cell death in peripheral lymph nodes without a depletion of circulating $CD4^+$ T cells. After the acute viremic stage, the plasma viral load declined earlier in the SHIV-TNF-inoculated monkeys than in the parental SHIV-NI-inoculated monkeys. SHIV-TNF was found to produce some immunity in macaque monkeys, leading to the elimination of SHIV. Based on these results, we propose that TNF-α contributes to the induction of an effective immune response rather than to the progression of disease at the early stage of HIV-1 infection.

Results

Virus load in rhesus macaques with SHIV-NI and SHIV-TNF

A recombinant SHIV was engineered to express TNF-α (SHIV-TNF) in place of *nef* in SHIV-NI (Fig. 1A). To investigate the in vivo properties of an SHIV-TNF, three rhesus monkeys (MM343, MM350, and MM351) were intravenously inoculated with 10^5 tissue culture 50% infectious dose ($TCID_{50}$) of SHIV-TNF, and two animals (MM346 and MM349) were inoculated with 10^5 $TCID_{50}$ of SHIV-NI as a control. All monkeys were viremic within 2 weeks post-inoculation (WPI) (Fig. 2A). This was also the case for two monkeys (MM287 and MM288) that were inoculated with same dose of SHIV-NI in a previous report (Enose et al., 2004). The plasma viral RNA loads were about the same in all SHIV-TNF- and SHIV-NI-inoculated monkeys, reaching a peak value of 10^4 RNA copies/ml during 1 to 2 WPI. Up-regulation of the plasma viral load in the SHIV-TNF-inoculated monkeys was not more than that in the SHIV-NI-inoculated monkeys.

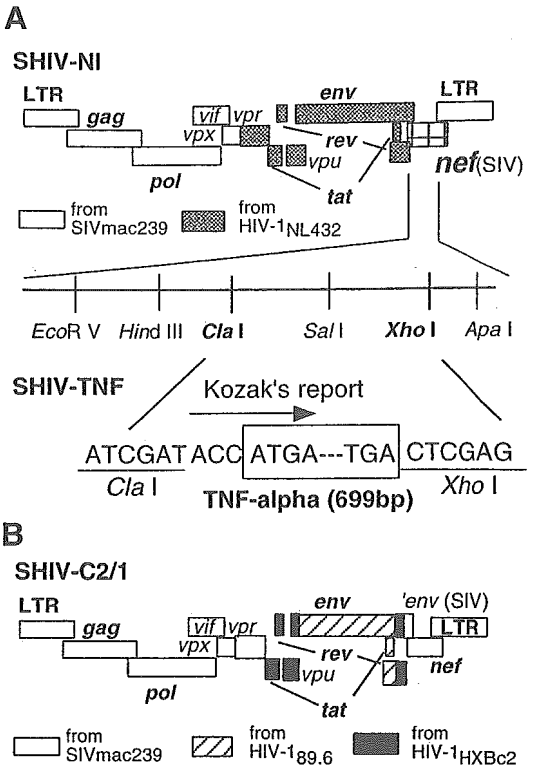

Fig. 1. Genetic structures of SHIVs used in this study. (A) Parental SHIV-NI and SHIV-TNF. SHIV-NI has some unique restriction enzyme sites in place of the *nef* gene of SHIV-NM3rN. SHIV-NM3rN was constructed from HIV-1 NL432 (dot regions) and SIV mac239 (white regions). In the SHIV-TNF, the *Cla*I and *Xho*I region of the parental SHIV-NI was replaced by the human TNF-α gene. The open reading frame including the initiation (ATG) and stop (TGA) codons of the TNF-α gene is shown in the box. The flanking sequence of the TNF-α initiation codon (ACCATGA) is an effective ribosomal initiation sequence based on Kozak's report (effective ribosomal initiation sequence: ANNATGN or GNNATGR). (B) Challenge virus SHIV-C2/1. SHIV-C2/1 (GenBank accession number AF217181) was generated by in vivo passage of SHIV-89.6 through cynomolgus monkeys. SHIV-89.6 was constructed from HIV-1 HXBc2, HIV-1 89.6, and SIV mac239.

However, the kinetics of the viral loads was different between the two groups. At the post-acute phase, the plasma viral loads declined earlier in the SHIV-TNF group (becoming undetectable at about 4 WPI) than in the SHIV-NI group (becoming undetectable at 6–8 WPI). After the acute viremic stage, the plasma virus load declined to undetectable levels earlier in the SHIV-TNF group than in the SHIV-NI group ($P < 0.05$ at 3 WPI).

Proviral DNAs in PBMCs from macaques infected with SHIV-TNF were isolated, and the stability of the inserted TNF-α gene in SHIV-TNF was studied by PCR with primer pairs that recognized the site where the TNF-α gene had been inserted. Due to the limited viral replication, proviral DNAs in PBMCs of the SHIV-TNF inoculated monkeys were detected up to 3 or 4 WPI. The full-length of the inserted TNF-α was observed in the proviral DNAs (Fig. 2B).

Lymphocyte phenotyping of PBMC and lymph nodes

After the infection, the number of peripheral $CD4^+$ lymphocytes remained within the normal level in both the

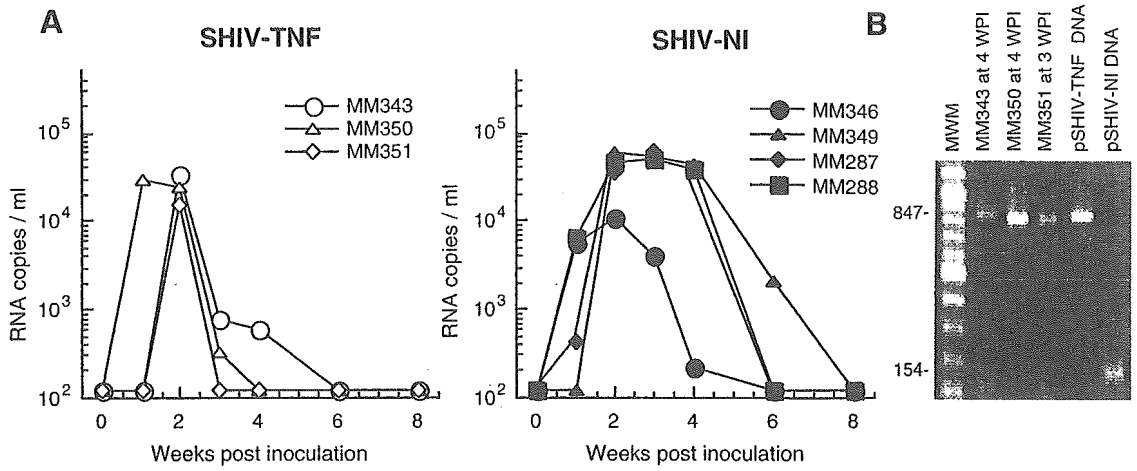

Fig. 2. Viral loads of SHIVs and TNF-α gene stability. (A) Viral RNA loads in plasma of monkeys inoculated with SHIV-TNF and SHIV-NI. Data for MM287 and MM288 are from a previous report (Enose et al., 2004). Plasma viral RNA loads were measured by RT-PCR. The detection limit of this assay was 1.2×10^2 copies/ml. (B) Stability of the inserted TNF-α gene in SHIV-TNF, as shown by PCR. DNA plasmids of SHIV-TNF (pSHIV-TNF DNA) and SHIV-NI (pSHIV-NI DNA) were used as the templates of the control. MWM, molecular weight markers of 100-bp ladder.

SHIV-NI- and SHIV-TNF-inoculated monkeys (Fig. 3A). No clinical changes were observed in any of the monkeys during the observation period. These results showed that SHIV-TNF did not cause an AIDS-like disease. No significant differences were observed between the SHIV-NI- and SHIV-TNF-inoculated monkeys in the cell surface markers of PBMCs. In contrast, the percentage of $CD20^+$ B cells in the lymph nodes changed dramatically in the SHIV-TNF-inoculated macaques after the inoculation of virus (Fig. 3B). After the inoculation of SHIV-TNF, development of germinal centers in the lymph nodes was observed with hematoxylin and eosin staining (data not shown). These data suggest that the inoculation of SHIV-TNF induced the activation of $CD20^+$ B cells in the lymph nodes at the early stage of the infection, without disturbing the immunological status.

Plasma levels of TNF-α and RANTES

We next examined the plasma levels of some cytokines by enzyme-linked immunosorbent assay (ELISA). The levels of TNF-α in the plasma of macaques infected with SHIV-TNF and SHIV-NI were below the detection limit (15.6 pg/ml) of the ELISA at all time points (data not shown).

TNF-α inhibited HIV-1 replication by inducing the production of CC-chemokines such as regulated-on-activation-normal-T-cell-expressed-and-secreted (RANTES) (Lane et al., 1999). To determine whether SHIV-TNF induces the expression of RANTES, plasma levels of RANTES were investigated (Fig. 3C). Interestingly, the plasma RANTES levels in the SHIV-TNF-infected monkeys were higher (about 3 times higher) than those in SHIV-NI-infected monkeys at 2 WPI, when the plasma viral load was about the same in the two groups. Plasma RANTES levels in the parental SHIV-NM3rN-inoculated monkeys (Kwofie et al., 2000) and two other SHIV-NI-inoculated monkeys (2.7 ng/ml for MM287 and 2.0 ng/ml for MM288, respectively, at 2 WPI) from our previous study were similar to those in the SHIV-NI-infected monkeys. The difference of the plasma RANTES levels between the SHIV-TNF-infected monkeys and the SHIV-NI-infected monkeys is statistically significant ($P < 0.05$ at 2 WPI). After 8 WPI, the plasma level of RANTES declined to the pre-infection level in all SHIV-TNF-infected monkeys.

Antibody titer

The humoral immune response was assessed with an HIV-1 particle agglutination assay. Induction of anti-HIV-1 antibodies was first detected in two of three SHIV-TNF-infected monkeys (MM343 and MM350) at 3 WPI (Fig. 3D). The antibody titers for the other SHIV-TNF-inoculated monkey (MM351), SHIV-NI-inoculated monkey, and the two SHIV-NI-infected monkeys in our previous experiment (MM287 and MM288) (data not shown) all slightly increased at 4 WPI. Although the data were not statistically significant ($P = 0.08$ at 3 WPI), the results showed that some SHIV-TNF-infected monkeys immediately developed an antiviral antibody response during the early stage of infection.

Induction of cell death in lymph nodes of SHIV-TNF-inoculated monkeys

TNF-α induces apoptosis of lymphocytes (Zheng et al., 1995). Spontaneous- or activation-induced ex vivo apoptosis of lymphocytes was reported in infections of HIV-1-related viruses (Gougeon et al., 1996; Iida et al., 2000; Reinberger et al., 1999). Thus, we investigated the induction of cell death in biopsy samples from lymph nodes by Annexin V assay and terminal deoxynucleotidyl transferase dUTP nick end-labeling (TUNEL) assay. In two of the SHIV-TNF-inoculated monkeys (MM343 and MM351), the percentages of lymphocytes undergoing cell death increased 24.2% and 17.5%, respectively, at 2 WPI (Fig. 4A). In the SHIV-NI-inoculated monkeys

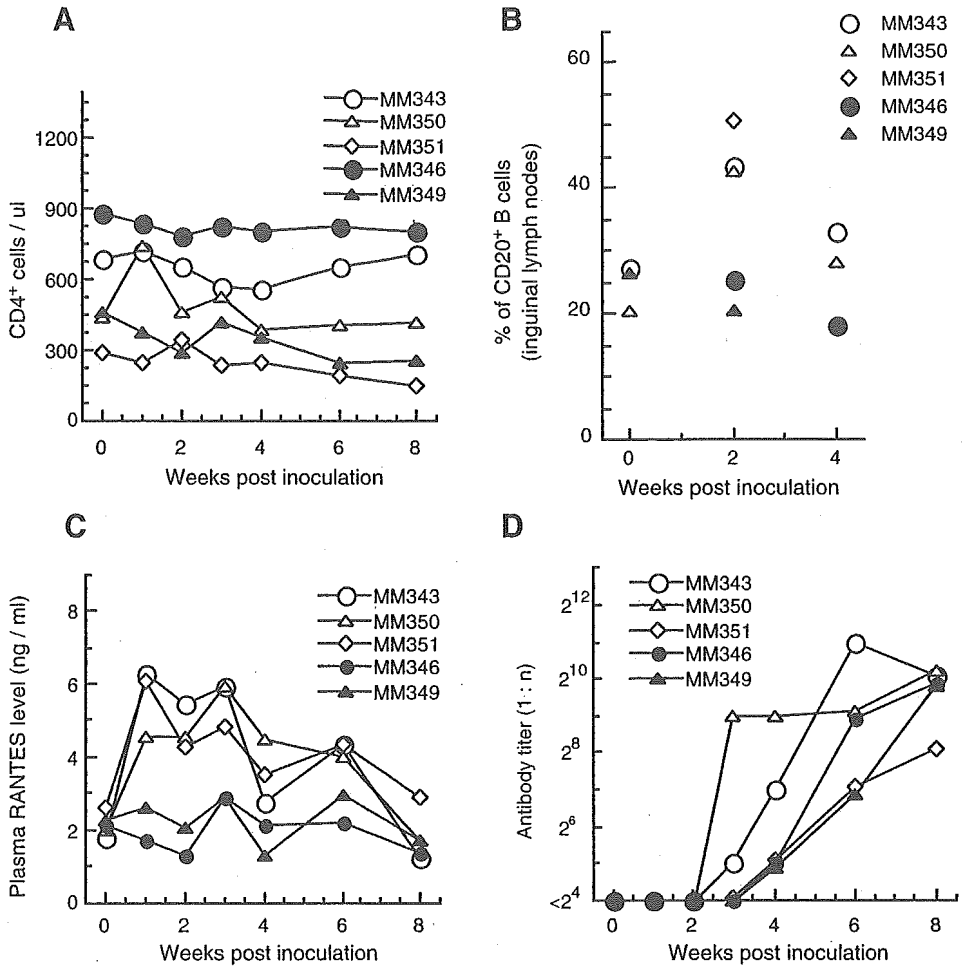

Fig. 3. Change in immune responses in rhesus monkeys after inoculation with SHIV-TNF (open symbols) and SHIV-NI (closed symbols). (A) $CD4^+$ T lymphocyte counts. Values were calculated from the percentage $CD3^+CD4^+$ cells measured by flow cytometry. The absolute number of lymphocytes was obtained by automated blood cell counter. (B) Percentage of $CD20^+$ B cells ($CD3^-CD20^+$ cells) in the inguinal lymph nodes. Data were not obtained for all monkeys at each time. (C) Plasma RANTES levels, as measured by ELISA. (D) Humoral immune responses, as expressed by anti-HIV-1 antibody titer. Antibody titer was analyzed by particle agglutination assay and is expressed as the maximum dilution of plasma to give a positive result.

(MM346 and MM349), the percentages of Annexin-V-positive lymphocytes after the virus inoculation remained at 4.1% and 7.5%, respectively, which were the pre-inoculation levels. The percentage of Annexin-V-positive cells in the lymph nodes was markedly higher in the SHIV-TNF-inoculated macaques than in the SHIV-NI-inoculated macaques. Induction of cell death in the SHIV-TNF group was also observed by the TUNEL assay (Fig. 4B). These results show that induction of cell death in inguinal lymph nodes in the SHIV-TNF group was significantly higher than that in SHIV-NI group, suggesting that TNF-α expressed by the SHIV-TNF-infected cells induced apoptosis in lymph nodes in the virus-inoculated monkeys.

Induction of antigen-specific lymphocyte proliferative responses in SHIV-TNF-inoculated macaques

To determine whether inoculation of the SHIV-TNF elicited antigen-specific lymphocytes in the animals, proliferative responses to SIV Gag were measured with PBMCs by uptake of 5-bromo-2′-deoxyuridine (BrdU). During the experimental period, antigen-specific T cell proliferation was induced especially in the SHIV-TNF-inoculated monkeys (Fig. 5A). Proliferative responses to Gag in the SHIV-TNF group were observed as early as 2 WPI. Subsets of proliferative lymphocytes were also characterized by combination of anti-BrdU and surface marker staining. In the SHIV-TNF-inoculated monkeys, the antigen-specific proliferative response was observed both in CD4-positive and in CD8-positive cells (Fig. 5B). These results show that antigen-specific T cell proliferation was induced markedly in the SHIV-TNF group at the early stage of infection.

The proliferative responses to a mitogen (Concanavalin A; ConA) were low or absent in the SHIV-NI-inoculated monkeys at 3 and 4 WPI, and then the response to ConA recovered to the normal level afterward (Fig. 5C). In contrast, the SHIV-TNF-infected macaques showed a continuous response to ConA.

Challenge with a pathogenic SHIV

To evaluate the protective effects provided by SHIV-TNF, monkeys were challenged intravenously with 10^5 $TCID_{50}$ of heterologous pathogenic SHIV-C2/1 KS661 (Fig. 1B) at 8 WPI.

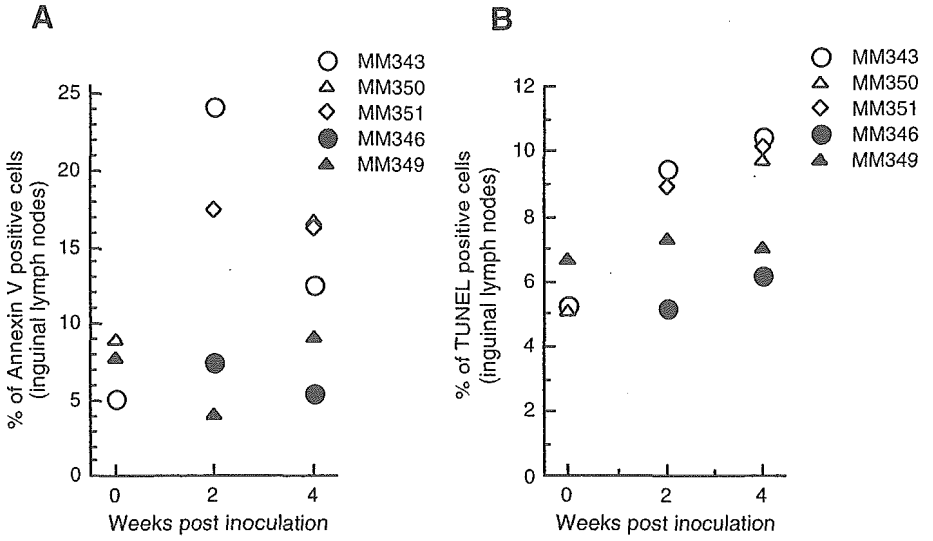

Fig. 4. Induction of cell death in inguinal lymph node mononuclear cells following infection with SHIV-TNF (open symbols) and SHIV-NI (closed symbols). Cells were collected at the indicated times and incubated for 24 h before analyses. (A) Percentage of Annexin-V-positive cells. (B) Percentage of fragmentation of chromosomal DNA, measured by flow cytometry with TUNEL assay. Data were not obtained for all monkeys at each time.

As controls, four naive monkeys (MM298, MM299, MM338, and MM339) were infected intravenously with the same dose (10^5 $TCID_{50}$) of SHIV-C2/1 KS661. Circulating $CD4^+$ lymphocytes decreased in all of the control monkeys, reaching less than 50 cells/μl in accordance with a previous report (Shinohara et al., 1999) (Fig. 6A). The viral RNA in the plasma of the control monkeys increased to above 10^7 copies/ml at 1 WPI and remained at a high level (Fig. 6B).

All of the monkeys in the SHIV-TNF group were more resistant to the challenge than the control monkeys. The circulating $CD4^+$ T cell counts were maintained in all SHIV-TNF-infected monkeys (Fig. 6A). The peak plasma virus loads in the SHIV-TNF group (10^5 and 10^6 copies/ml) were two orders of magnitude lower than those of the naive SHIV-C2/1 KS661-inoculated monkeys (Fig. 6B). Interestingly, the plasma virus loads in two of the three SHIV-TNF-inoculated monkeys (MM343 and MM351) rapidly declined to below the detection limit at 4 weeks post-challenge (WPC). The peak plasma viral load of one of the SHIV-NI-infected monkeys (MM349; 10^7 copies/ml) was similar to that of the control monkeys. The circulating $CD4^+$ T cell count in MM349, an SHIV-NI-infected monkey, remained within the normal range in spite of a transient but intense viremia in the plasma (Fig. 6A). These results show that all SHIV-TNF-inoculated monkeys were partially protected from challenge, with a pathogenic SHIV having a heterologous HIV-1 Env. Moreover, some SHIV-TNF-infected monkeys may have immediately eliminated the heterologous challenge virus in the plasma.

Discussion

The aim of this study was to clarify the role of TNF-α against HIV-1-related virus infection in an SHIV-macaque model. For this purpose, we have genetically engineered an SHIV to express the TNF-α gene so that, when viral transcription occurs, TNF-α will also be produced locally. We compared the in vivo properties of macaques infected with SHIV-TNF with those of its parental SHIV-NI. Although the number of animals examined was small, some virologic and immunologic parameters in macaques infected with SHIV-TNF and with SHIV-NI were different between the groups.

In a previous in vitro study, SHIV-TNF was found to replicate better than SHIV-NI does in macaque PBMCs (Haga et al., 2002). In vivo, however, the plasma viral loads were about the same in the two groups during acute infection. The plasma viral loads in the SHIV-TNF-inoculated monkeys dramatically declined to undetectable levels after the acute phase of the infection, while the viral loads of the parental SHIV-NI-inoculated monkey declined gradually. The spread of the virus was suppressed in the animals infected with SHIV-TNF. Suppression of the virus may have been due to cell deaths in the lymph nodes from the SHIV-TNF-inoculated monkeys. An efficient induction of cell death, through the TNF/TNF-receptor (TNFR) pathway, could restrict virus replication by eliminating virus-infected cells (Herbein and O'Brien, 2000). HIV-1-infected lymphocytes treated with TNF-α underwent apoptosis resulting in a decreased HIV-1 replication, suggesting that cell death helps to inhibit the spread of HIV-1 (Lazdins et al., 1997). Insertion of the TNF-α gene in the SHIV induced a rapid cell death at the site where virus replicates, with a subsequent reduction of the spread of the virus.

A cytokine-expressing SIV was observed to lose the cytokine gene within several weeks in vivo (Gundlach et al., 1997). In our study, the proviral DNA isolated from PBMCs of macaques inoculated with SHIV-TNF during the viremia retained full-length TNF-α inserts. Due to the limited and local nature of viral replication, we could not detect TNF-α in the plasma of animals inoculated with SHIV-TNF. However, the TNF-α gene inserted in SHIV-TNF was stable in vivo during the viremia.

In vitro studies have suggested that pretreatment of macrophages with TNF-α helps to protect them against HIV-

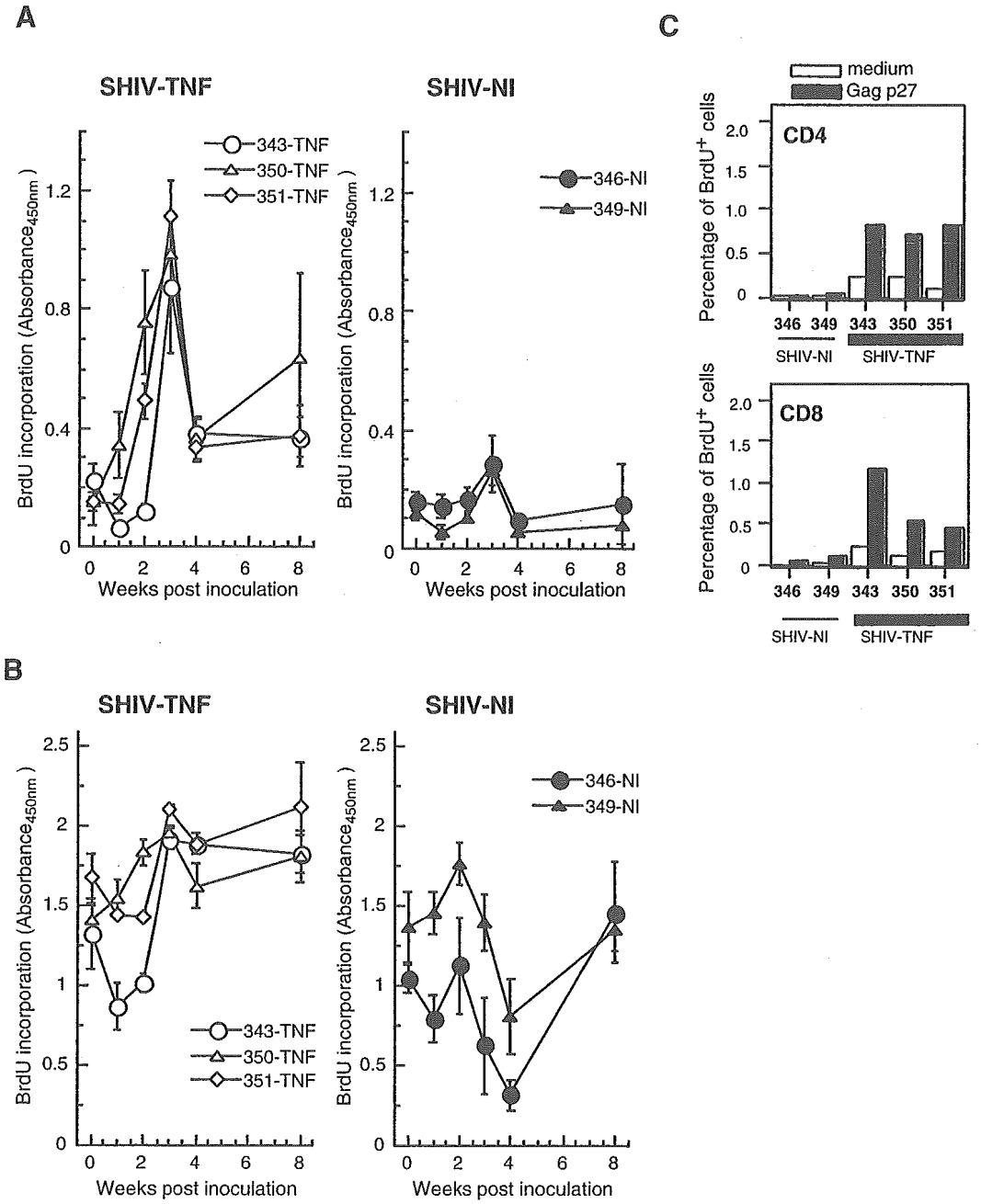

Fig. 5. T cell proliferation in SHIV-TNF- and SHIV-NI-inoculated rhesus monkeys in response to an SHIV-specific antigen (SIV Gag; A and C) or a mitogen (ConA; B). (A, B) Lymphocytes proliferation, as measured by BrdU uptake, in response to SIV Gag (A) and ConA (B). Data are expressed as the mean of triplicate determinations ± SEM. (C) Percentage of the SIV Gag-specific proliferated cells (solid bars) and unstimulated cells (open bars) at 6 WPI that were $CD4^+$ or $CD8^+$ cells, as measured by flow cytometry.

1. This is largely because TNF-α induces the secretion of CC-chemokines such as macrophage inflammatory protein-1 alpha (MIP-1α), beta (MIP-1β), and RANTES (Herbein and Gordon, 1997; Lane et al., 1999). In this experiment, an increase in RANTES production was observed in the SHIV-TNF-inoculated monkeys. At the peak, the plasma level of RANTES was three times higher in the SHIV-TNF-infected monkeys than in the SHIV-NI-infected monkeys. RANTES is known to suppress a CC-chemokine receptor 5 (R5)-tropic HIV-1 in vitro (Alkhatib et al., 1996; Cocchi et al., 1995), but not a CXCR4 (X4)-tropic virus including HIV-1 NL432, the source of the *env* gene of SHIV-TNF. Therefore, the high RANTES production probably did not limit the replication of SHIV-TNF in this study. Many cohort studies have suggested that an increase of RANTES inhibits the development of AIDS (Aukrust et al., 1998; Garzino-Demo et al., 1999). Furthermore, RANTES regulates cell migration to the site of inflammation. The appropriate expression of RANTES can improve the host immune response against HIV-1. Together, our result suggests that TNF-α helps to induce an effective immune response against HIV-1 by mediating the expression of the CC-chemokine RANTES.

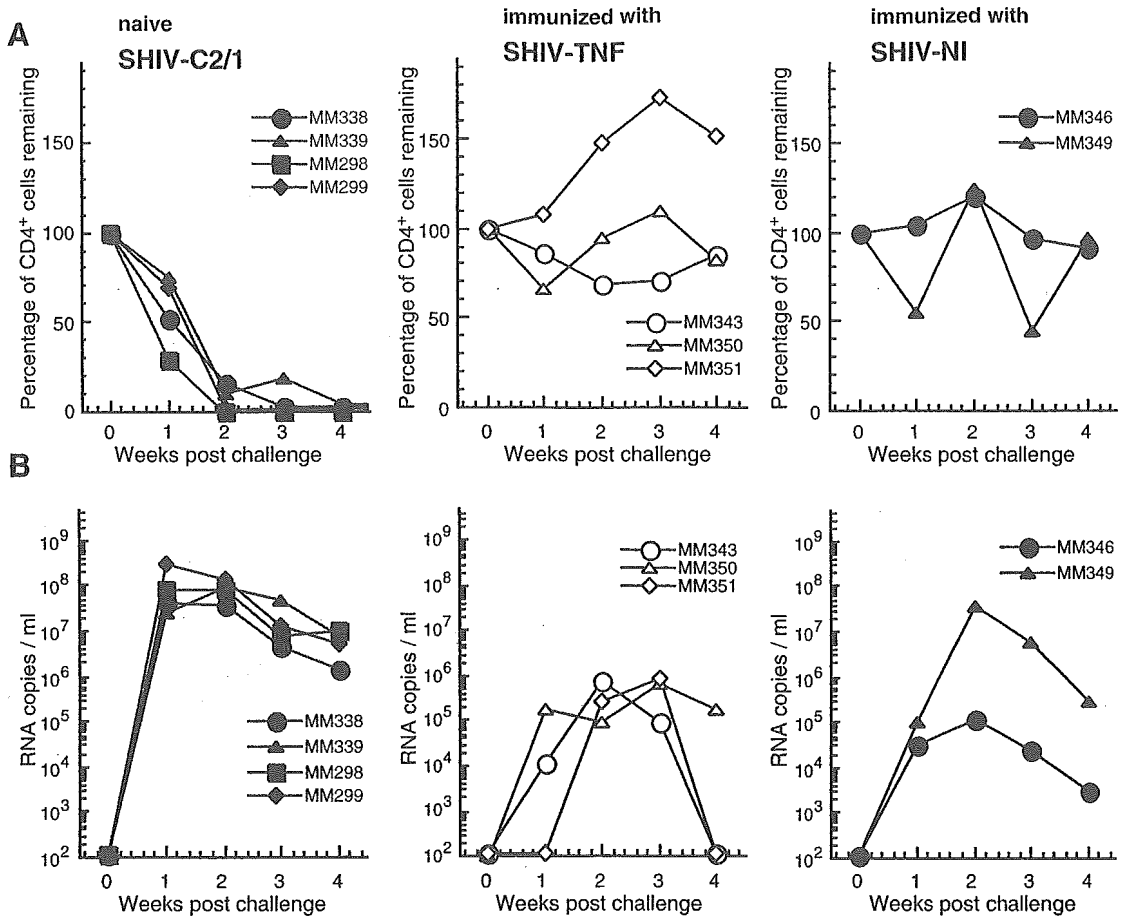

Fig. 6. Change in the number of circulating $CD4^+$ T cells (A) and SHIV-C2/1-specific viral RNA loads (B) of the SHIV-NI- and SHIV-TNF-inoculated monkeys after SHIV-C2/1 challenge. Values are expressed as a percentage of the pre-challenge values of each monkey. Plasma viral RNA loads after the heterologous pathogenic SHIV (SHIV-C2/1) challenge were measured by RT-PCR. The detection limit of this assay was 1.2×10^2 copies/ml. Left panels show results for naive SHIV-C2/1-inoculated monkeys (MM338, MM339, MM298, and MM299).

Another finding of the present study is that the inoculation of SHIV-TNF induced a remarkable antigen-specific T cell proliferation at the early stage of infection. In human, TNF-α enhances mitogen- and antigen-induced T cell proliferation (Tartaglia et al., 1993; Yokota et al., 1988). TNF-α produced by HIV-1-infected macrophages has been reported to stimulate bystander T cell proliferation (Godard and Chermann, 1998). Our results suggest that the co-expression of viral antigen and TNF-α stimulates antigen-specific T cell proliferation. Antigen-specific T cell proliferation is important for the control of AIDS pathogenesis. Proliferation of HIV-1 p24-specific $CD4^+$ T cells, which has been associated with control of acute infection and delayed disease progression, has been shown to inhibit the replication of HIV-1 (Rosenberg et al., 1997). Therefore, TNF-α appears to induce effective antigen-specific immune responses of lymphocytes, which may help to prevent the progression of disease.

The proliferative responses to a mitogen (ConA) were low or absent in parental SHIV-NI-inoculated monkeys during the period from 3 WPI to 4 WPI. Mitogen-stimulated proliferation of lymphocytes was also found to be inhibited during the acute stage of HIV-1 infection (Cooper et al., 1988; Pedersen et al., 1990). A transient impairment of proliferative response to mitogens has been correlated with host immune suppression. A decrease in the level of TNF-α in a virus infection was found to suppress mitogen- and antigen-stimulated lymphocyte proliferation (Griffin et al., 1994), and mitogen- and antigen-stimulated lymphocyte proliferation was restored by addition of exogenous TNF-α (Kasahara et al., 2003). In the present study, the SHIV-TNF-infected macaques showed a continuous proliferative response to ConA during the observation period. These results suggest that co-expression of TNF-α by a genetically engineered virus sustains the virus-induced immune suppression.

Most studies of the relationship between TNF-α and HIV-1 infection have focused on patients at the AIDS stage. TNF-α has been implicated in the progression of AIDS because of the possibilities that TNF-α enhances HIV-1 replication (Folks et al., 1989; Poli et al., 1990) and induces apoptosis of lymphocytes (Badley et al., 1997; Herbein et al., 1998). In this study, SHIV-TNF replicated transiently in inoculated monkeys, and the number of peripheral $CD4^+$ lymphocytes remained within the normal level in all SHIV-TNF-inoculated monkeys, despite the induction of cell death in inguinal lymph nodes. Although we cannot exclude the possibility that TNF-α contributes to disease progression in the late stage of

infections, the SHIV-TNF-inoculated macaques did not develop AIDS-like disease during the experimental period.

At the early stage of HIV-1 infection, expression of TNF-α also increased in some individuals (von Sydow et al., 1991), which was considered to contribute to the inflammatory response seen in acute HIV-1 infection. The present results demonstrate that SHIV-TNF induced the expression of RANTES, antigen-specific T cell proliferation, and rapid cell death with a subsequent reduction of plasma viral loads at the early stage of infection. The appearance of TNF-α activates the virus-specific immune response, which contributes to viral clearance. Therefore, at the early stage of HIV-1 infection, we propose that TNF-α plays a role in the induction of an effective immune response, rather than in the progression of the disease.

The immune responses induced by an attenuated virus can increase the immunity to a pathogenic virus. We previously reported that macaque monkeys immunized with the parental SHIV-NI were partially protected from a challenge with a heterologous pathogenic SHIV (Enose et al., 2002; Ui et al., 1999). In the present study, the monkeys that received the inoculation of SHIV-TNF were partially protected from a challenge with a heterologous pathogenic SHIV-C2/1. The immune response induced by the inoculation of SHIV-TNF helped to suppress the spread of a heterologous pathogenic SHIV. It is noteworthy that the challenge virus load rapidly declined to below the detection limit in some SHIV-TNF-inoculated monkeys.

In general, the immunogenicity of live-attenuated vaccines tends to increase with increasing virulence (Johnson and Desrosiers, 1998). Therefore, in attenuating a live virus, there is a trade-off between safety and immunogenicity. A good way to overcome this problem is to genetically engineer a virus to co-express an anti-viral agent such as a cytokine adjuvant. The expression of an inserted cytokine gene from a genetically engineered vaccine virus provides adjuvant effects locally at the site of virus replication. Several studies have demonstrated that insertion of a cytokine in a gene-deleted live-attenuated SIVs could boost the immunogenicity of the viruses and enhance its protection ability (Giavedoni et al., 1997; Stahl-Hennig et al., 2003). For the immune adjuvant effect of TNF-α, a combination of cytokines including TNF-α enhanced cellular immune responses resulting in a more effective immune-modulating effect against HIV-1 in the rodent model (Ahlers et al., 1997, 2003). In this study, SHIV-TNF induced antiviral immune responses in the virus-inoculated monkeys that subsequently rapidly cleared the virus. The rapid viral clearance and enhanced immunogenicity may improve the safety of a live-attenuated virus vaccine candidate because these responses will reduce the risks of residual pathogenicity, reversion to a pathogenic virus, and recombination of the vaccine virus with the challenge virus (Baba et al., 1999; Gundlach et al., 2000). These results raise the possibility that a genetically engineered anti-viral agent, such as TNF-α, can improve the safety and immunogenicity of an attenuated live virus vaccine.

In conclusion, we showed that SHIV-TNF induces (i) rapid clearance of virus after the acute viremic stage, (ii) cell death in peripheral lymph nodes without depletion of circulating $CD4^+$ T cells, (iii) up-regulation of the plasma level of the chemokine RANTES, (iv) antigen-specific proliferation of lymphocytes, and (v) protection against a pathogenic SHIV-C2/1 challenge. These findings suggest that TNF-α contributes to the induction of an effective immune response at the early stage of HIV-1 infection and that a genetically engineered virus to co-express the TNF-α gene can be useful for studying the immune-modulating effect of TNF-α in HIV-1-related infections.

Materials and methods

Viruses and animals

SHIV-NI and SHIV-TNF were constructed from SHIV-NM3rN as previously described (Fig. 1A) (Haga et al., 2002). A heterologous pathogenic SHIV-C2/1 KS661 was used for the challenge virus (Fig. 1B). SHIV-C2/1 KS661 is a molecular clone derived from SHIV-C2/1 and causes rapid $CD4^+$ T cell depletion (GenBank accession number AF217181) (Shinohara et al., 1999). The *env* gene of SHIV-C2/1 was derived from HIV-1 89.6 and is antigenically different from the *env* gene of SHIV-NI and SHIV-TNF. Virus stocks were prepared with the $CD4^+$ human T cell line M8166 (a subclone of C8166) as described elsewhere (Haga et al., 2002). Five female rhesus monkeys (*Macaca mulatta*) were maintained in accordance with regulations approved by the Institutional Animal Care and Use Committee of the Institute for Virus Research, Kyoto University, and were housed in single cages within a biosafety level 3 facility. Blood samples were collected under anesthesia with ketamine hydrochloride.

Inoculation of rhesus monkeys with SHIV and sample collection

To investigate the in vivo properties of SHIV-TNF and SHIV-NI, three rhesus monkeys (MM343, MM350, and MM351) were inoculated intravenously with 10^5 $TCID_{50}$ of SHIV-TNF, and two monkeys (MM346 and MM349) were inoculated with 10^5 $TCID_{50}$ of SHIV-NI. Blood samples were phenotypically characterized on a FACScan flow cytometer (Becton Dickinson, San Jose, CA) and were separated into plasma and PBMCs with lymphocyte separation solution (Nacalai Tesque, Inc. Kyoto, Japan). Inguinal lymph nodes were obtained from these animals by biopsy at 2 and 4 WPI and before infection. Single-cell suspensions were prepared from the inguinal lymph nodes with a 100 μm nylon cell strainer (Becton Dickinson). Part of the inguinal lymph nodes was fixed in 4% paraformaldehyde and embedded in paraffin for histopathologic analysis. To evaluate the protective effects provided by the SHIV-TNF or SHIV-NI inoculation, all monkeys were challenged intravenously with 10^5 $TCID_{50}$ of SHIV-C2/1 KS661 at 8 WPI.

Plasma viral RNA loads

Plasma viral RNA loads were determined by quantitative RT-PCR (Enose et al., 2002; Suryanarayana et al., 1998). The

plasma viral loads of SHIV-NI, SHIV-TNF, and the challenge virus were differentially evaluated with primer pairs specific to SHIV-NM3rN and SHIV-C2/1, respectively (Enose et al., 2004). These reactions were performed with a Prism 7700 Sequence Detector (Applied Biosystems, Foster City, CA) and analyzed using the manufacturer's software. The viral RNA in the plasma samples was quantified based on the copy number of the standard samples.

Isolation of proviral DNA

Proviral DNA was extracted from 1×10^6 PBMCs and amplified by PCR with primers specific for the *nef* region. Cellular DNAs were extracted from PBMCs of the inoculated monkeys using DNeasy tissue kits (QIAGEN, Hilden, Germany) according to the manufacturer's recommendations. The proviral DNA fragments covering the inserted TNF-α gene in SHIV-TNF were amplified from each cellular DNA by PCR as previously described (Haga et al., 2000). The lengths of DNA fragments generated by this reaction were 847 bp for the SHIV containing the intact TNF-α gene and 154 bp for SHIV-NI.

Determination of TNF-α and RANTES

Plasma samples were thawed and centrifuged at $10,000 \times g$ for 10 min at 4 °C. TNF-α levels in the plasma were determined by ELISA using a Quantikine Human TNF-α ELISA kit (R&D Systems, Inc., Minneapolis, MN) and a Monkey TNF-α ELISA kit (Biosource International, Inc., Camarillo, CA). Plasma RANTES concentration was measured using a human RANTES ELISA kit (R&D Systems), which is known to cross-react with rhesus RANTES (Kwofie et al., 2000).

Lymphocyte analysis

Blood samples and inguinal lymph node suspensions were stained with combinations of the following monoclonal antibodies (MAbs): anti-human CD4 (NU-TH/I, Nichirei, Tokyo, Japan), anti-human CD8 (Leu-2a, Becton Dickinson), anti-monkey CD3 (FN18, Biosource International), anti-human CD20 (Leu-16, Becton Dickinson), anti-human CD29 (4B4; Beckman Coulter, Miami, FL), anti-human CD14 (RMO52; Beckman Coulter), anti-human CCR5 (3A9; Pharmingen, San Diego, CA), anti-human CXCR4 (12G5; Pharmingen), and anti-Ki67 antigen (Ki-67, DAKO, Glostrup, Denmark). Ten thousand events per sample were acquired by a FACScan flow cytometer, and data were analyzed by CellQuest software (Becton Dickinson) and FlowJo software (TreeStar, San Carlos, CA). Absolute lymphocyte counts in the blood were determined with an automated blood cell counter (F-820; Sysmex, Kobe, Japan).

Analysis of cell death

The percentages of lymphocytes undergoing cell death were determined by Annexin V assay and TUNEL assay. Mononuclear cells (1×10^6) from the blood and lymph nodes were cultured for 24 h ex vivo in 24-well culture plates in complete RPMI medium (RPMI 1640 with 10% heat-inactivated fetal calf serum) per milliliter at 37 °C. In the Annexin V assay, a MEBCYTO apoptosis kit (MBL, Nagoya, Japan) was used according to the manufacturer's instructions. As another assay of cell death, fragmentation of chromosomal DNA was detected with a TUNEL assay. An APO-BrdU kit (Pharmingen) was used according to the manufacturer's instructions. The cells were then analyzed by flow cytometry.

Proliferation assays

Lymphocyte proliferation was measured by incorporation of BrdU into the stimulated lymphocytes. PBMCs (2×10^5) were cultured in a 96-well plate in complete RPMI medium. The recombinant viral proteins of SIV Gag (SIVmac251 p27; 5.0 μg/ml; Advanced Biotechnologies, Inc., Columbia, MD) were used for antigen-specific stimulation. Concanavalin A (ConA; 0.5 μg/ml; Sigma, St. Louis, MO) was used for polyclonal stimulation. The plates were incubated for 72 h at 37 °C. After the incubation, the cells were cultured for another 24 h in the presence of BrdU. Then, lymphocyte proliferation was measured using a cell proliferation ELISA kit (Roche Diagnostics, Basel, Switzerland) and a BrdU-Flow kit (Pharmingen) following the manufacturer's recommendations. In the ELISA, the absorbance of the incorporated BrdU was measured by a microplate reader at 450 nm. The experiment was performed in triplicate. In another cell proliferation assay, to characterize the lymphocyte subsets in the proliferated cells, cells were stained for surface markers with MAb CD4-PE (Nichirei) and CD8-PerCP (Becton Dickinson). The cells were stained with MAb BrdU-FITC after fixation and permeabilization and then analyzed by flow cytometry. Proliferation responses to the antigens were considered positive if the stimulation index (SI = titers for antigen-stimulated wells / titers for control wells without antigens) exceeded 2.0 (Ahmed et al., 2002).

Determination of anti-SHIV antibody titers

Anti-SHIV antibody titers in the plasma of the monkeys were determined using a commercial particle agglutination test kit (Genedia HIV-1/2, Fujirebio Inc., Tokyo, Japan). The samples were serially two-fold diluted and assayed following the manufacturer's recommendations. The end-point titer was determined as the highest dilution to give a positive result.

Statistical analysis

Differences between the groups of plasma viral RNA loads, plasma RANTES level, and anti-SHIV antibody titers in the plasma were compared by statistical analysis using the Mann–Whitney *U* test; *P* values <0.05 were considered statistically significant.